united nations
educational, scientific
and cultural
organization

international atomic
energy agency

the
abdus salam
international centre for theoretical physics

SMR.1092 - 2

SUMMER SCHOOL IN HIGH ENERGY PHYSICS AND COSMOLOGY

29 June - 17 July 1998

INTRODUCTION TO THE PHYSICS OF HIGGS BOSONS

S. DAWSON
Physics Department
Brookhaven National Laboratory
Upton, NY 11973
USA

Please note: These are preliminary notes intended for internal distribution only.

BROOKHAVEN NATIONAL LABORATORY

November 1994 BNL -61012

INTRODUCTION TO THE PHYSICS OF HIGGS BOSONS*

S. Dawson

Physics Department, Brookhaven National Laboratory, Upton, NY 11973

* Lectures given at the 1994 Theoretical Advanced Study Institute, Boulder, CO, May 30 – June 23, 1994

INTRODUCTION TO THE PHYSICS OF HIGGS BOSONS

S. Dawson
Physics Department,
Brookhaven National Laboratory,
Upton, NY 11973

Abstract

A basic introduction to the physics of the Standard Model Higgs boson is given. We discuss Higgs boson production in e^+e^- and hadronic collisions and survey search techniques at future accelerators. The Higgs bosons of the minimal SUSY model are briefly considered. Indirect limits from triviality arguments, vacuum stability and precision measurements at LEP are also presented.

Lectures given at the 1994 Theoretical Advanced Study Institute, Boulder, CO., May 30 -June 23, 1994

Contents

The search for the Higgs boson has become the holy grail of all particle accelerators. In the simplest version of the electroweak theory, the Higgs boson serves both to give the W and Z bosons their masses and to give the fermions mass. It is thus a vital part of the theory. In these lectures, we will introduce the Higgs boson of the Standard Model of electroweak interactions.[1] We discuss the production of the Higgs boson in both e^+e^- collisions and hadronic interactions and survey search techniques in the various Higgs mass ranges.[2]

Section 1 contains a derivation of the Higgs mechanism, with particular emphasis on the choice of gauge. In Section 2 we discuss Higgs production in e^+e^- collisions and describe the current LEP bounds on the Higgs mass. Hadronic production of the Higgs boson through gluon fusion and potential discovery channels at the LHC are the subjects of Section 3. Section 4 contains a derivation of the effective W approximation and a discussion of Higgs production through vector boson fusion at the LHC.

Suppose the Higgs boson is not discovered in an e^+e^- collider or at the LHC? Does this mean the Standard Model with a Higgs boson must be abandoned? In Section 5, we discuss the implications of a very heavy Higgs boson, ($M_H >> 700\ GeV$). Finally, in Section 6, we present indirect limits on the Higgs boson mass from triviality arguments, vacuum stability and precision e^+e^- measurements. Section 7 contains a list of some of the objections which many theorists have to the minimal standard model with a single Higgs boson. One of the most popular alternatives to the minimal Standard Model is to make the theory supersymmetric, which is discussed in Section 8. We present a lightning review of those aspects of supersymmetric theories which are relevant for Higgs boson phenomenology. We end with some conclusions in Section 9.

1 The Higgs Mechanism

1.1 Abelian Higgs Model

The central question of electroweak physics is :"Why are the W and Z boson masses non-zero?". The measured values, $M_W = 80\ GeV$ and $M_Z = 91\ GeV$ are far from zero and cannot be considered as small effects. To see that this is a problem, we consider a $U(1)$ gauge theory with a single gauge field, the photon. The Lagrangian is simply[3]

$$\mathcal{L} = -\frac{1}{4}F_{\mu\nu}F^{\mu\nu}, \tag{1}$$

where

$$F_{\mu\nu} = \partial_\nu A_\mu - \partial_\mu A_\nu. \tag{2}$$

The statement of local $U(1)$ gauge invariance is that the Lagrangian is invariant under the transformation:$A_\mu(x) \rightarrow A_\mu(x) - \partial_\mu\eta(x)$ for any η. Suppose we now add a mass

term to the Lagrangian,

$$\mathcal{L} = -\frac{1}{4}F_{\mu\nu}F^{\mu\nu} + \frac{1}{2}m^2 A_\mu A^\mu. \tag{3}$$

It is easy to see that the mass term violates the local gauge invariance. Hence it is gauge invariance that requires the photon to be massless.

We can extend the model by adding a single complex scalar field,

$$\phi \equiv \frac{1}{\sqrt{2}}(\phi_1 + i\phi_2). \tag{4}$$

The Lagrangian is now,

$$\mathcal{L} = -\frac{1}{4}F_{\mu\nu}F^{\mu\nu} + \mid D_\mu\phi \mid^2 - V(\phi), \tag{5}$$

where

$$\begin{aligned} D_\mu &= \partial_\mu - ieA_\mu \\ V(\phi) &= \mu^2 \mid \phi \mid^2 + \lambda(\mid \phi \mid^2)^2. \end{aligned} \tag{6}$$

$V(\phi)$ is the most general renormalizable potential allowed by the $U(1)$ invariance.

This Lagrangian is invariant under $U(1)$ rotations, $\phi \rightarrow e^{i\theta}\phi$ and under local gauge transformations:

$$\begin{aligned} A_\mu(x) &\rightarrow A_\mu(x) - \partial_\mu\eta(x) \\ \phi(x) &\rightarrow e^{-ie\eta(x)}\phi(x). \end{aligned} \tag{7}$$

(8)

There are two possibilities for the theory.[1] If $\mu^2 > 0$ then the potential has the shape shown in Fig. 1 and preserves the symmetry of the Lagrangian. The state of lowest energy is that with $\phi = 0$, the vacuum state. The theory is simply quantum electrodynamics with a massless photon and a charged scalar field ϕ with mass μ.

The alternative scenario is more interesting. In this case $\mu^2 < 0$ and the potential can be written as

$$V(\phi) = -\mid \mu \mid^2 \mid \phi \mid^2 + \lambda(\mid \phi \mid^2)^2, \tag{9}$$

which has the Mexican hat shape shown in Fig. 2. In this case the minimum energy state is not at $\phi = 0$ but rather at

$$\langle\phi\rangle = \sqrt{-\frac{\mu^2}{2\lambda}}. \tag{10}$$

$\langle\phi\rangle$ is called the vacuum expectation value (VEV) of ϕ. Note that the direction in which the vacuum is chosen is arbitrary, but it is conventional to choose it to lie along the direction of the real part of ϕ as shown in Fig. 2. It is convenient to write ϕ as

$$\phi \equiv \frac{1}{\sqrt{2}}e^{i\frac{\chi}{v}}\Big(v + H\Big), \tag{11}$$

[1] We assume $\lambda > 0$.

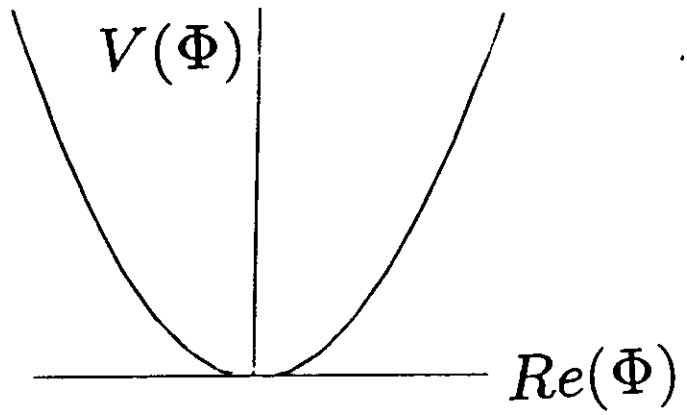

Figure 1: Scalar potential with $\mu^2 > 0$.

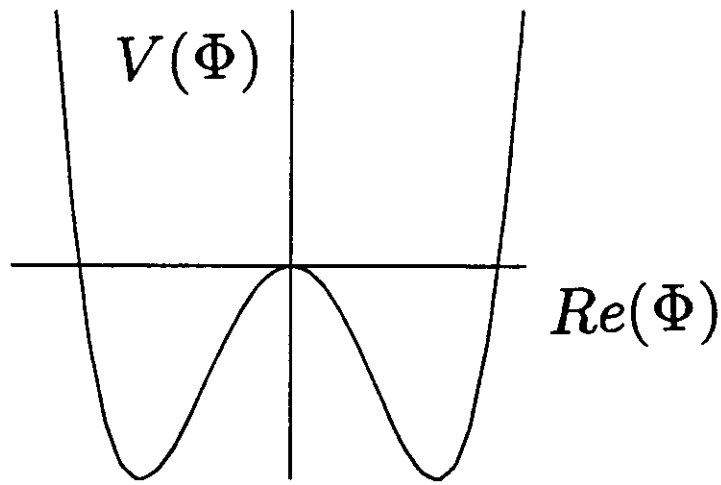

Figure 2: Scalar potential with $\mu^2 < 0$.

where χ and H are real fields which have no VEVs. If we substitute Eq. 11 back into the original Lagrangian we find the interactions in terms of the fields with no VEVs,

$$\begin{aligned}\mathcal{L} &= -\frac{1}{4}F_{\mu\nu}F^{\mu\nu} - evA_\mu\partial^\mu\chi + \frac{e^2v^2}{2}A_\mu A^\mu \\ &\quad +\frac{1}{2}\Big(\partial_\mu H\partial^\mu H + 2\mu^2H^2\Big) + \frac{1}{2}\partial_\mu\chi\partial^\mu\chi \\ &\quad +(H,\ \chi \text{ interactions}).\end{aligned} \tag{12}$$

Eq. 12 describes a theory with a photon of mass $M_A = ev$, a scalar field H with mass-squared $-2\mu^2 > 0$, and a massless scalar field χ. The mixed $\chi - A$ propagator is confusing however. This term can be removed by making a gauge transformation:

$$A'_\mu \equiv A_\mu - \frac{1}{ev}\partial_\mu\chi. \tag{13}$$

After making the gauge transformation of Eq. 13 the χ field disappears from the theory and we say that it has been "eaten" to give the photon mass. The χ field is often called a Goldstone boson.[4] In the gauge of Eq. 13 the particle content of the theory is apparent; a massive photon and a scalar field H. The field H is called a Higgs boson. The Higgs mechanism can be summarized by saying that the spontaneous breaking of a gauge theory by a non-zero VEV results in the disappearance of a Goldstone boson and its transformation into the longitudinal component of a massive gauge boson.

It is instructive to count the degrees of freedom (dof). Before the spontaneous symmetry breaking there was a massless photon (2 dof) and a complex scalar field (2 dof) for a total of 4 degrees of freedom.[2] After the spontaneous symmetry breaking there is a massive photon (3 dof) and a real scalar, H, (1 dof) for the same total degrees of freedom.

At this point let us make an aside about the gauge dependance of these results. The gauge choice above with the transformation $A'_\mu = A_\mu - \frac{1}{ev}\partial_\mu\chi$ is called the unitary gauge. This gauge has the advantage that the particle spectrum is obvious and there is no χ field. The unitary gauge however has the disadvantage that the vector propagator, $\Delta_{\mu\nu}(k)$, has bad high energy behaviour,

$$\Delta_{\mu\nu}(k) = -\frac{i}{k^2 - M_A^2}\Big(g_{\mu\nu} - \frac{k^\mu k^\nu}{M_A^2}\Big). \tag{14}$$

In the unitary gauge, scattering cross sections have contributions which grow with powers of k^2 (such as k^4, k^6, etc.) which cannot be removed by the conventional mass, coupling constant, and wavefunction renormalizations. More convenient gauges are the so-called R_ξ gauges which are obtained by adding the gauge fixing term to the Lagrangian,[5]

$$\mathcal{L}_{GF} = -\frac{1}{2\xi}\Big(\partial_\mu A^\mu + \xi ev\chi\Big)^2. \tag{15}$$

[2]Massless gauge fields have 2 transverse degrees of freedom, while a massive gauge field has an additional longitudinal degree of freedom.

Different choices for ξ correspond to different gauges. In the limit $\xi \to \infty$ the unitary gauge is recovered. Note that the cross term in Eq. 15 cancels the mixed $\chi\partial_\mu A^\mu$ term of Eq. 12. The gauge boson propagator in R_ξ gauge is given by

$$\Delta_{\mu\nu}(k) = -\frac{i}{k^2 - M_A^2}\left(g_{\mu\nu} - \frac{(1-\xi)k_\mu k_\nu}{k^2 - \xi M_A^2}\right). \tag{16}$$

In the R_ξ gauges the χ field is part of the spectrum and has mass $M_\chi^2 = \xi M_A^2$. Feynman gauge corresponds to the choice $\xi = 1$ and has massive Goldstone bosons, while Landau gauge has $\xi = 0$ and massless Goldstone bosons with no coupling to the physical Higgs boson. The Landau gauge is often the most convenient for calculations involving the Higgs boson since there is no coupling to the unphysical χ field.

1.2 Weinberg-Salam Model

It is now straightforward to obtain the usual Weinberg-Salam model of electroweak interactions.[6] Here we present a quick overview of the model with emphasis on those aspects relevant for Higgs physics. Further details can be found in the lectures of Peccei at this school.[7] The Weinberg- Salam model is an $SU(2)_L \times U(1)_Y$ gauge theory containing 3 $SU(2)$ gauge bosons, W_μ^i, and one $U(1)$ gauge boson, B_μ, with a kinetic energy term,

$$\mathcal{L}_{\rm KE} = -\frac{1}{4}W^i_{\mu\nu}W^{\mu\nu i} - \frac{1}{4}B_{\mu\nu}B^{\mu\nu} \tag{17}$$

where

$$\begin{aligned} W^i_{\mu\nu} &= \partial_\nu W^i_\mu - \partial_\mu W^i_\nu + g\epsilon^{ijk}W^j_\mu W^k_\nu \\ B_{\mu\nu} &= \partial_\nu B_\mu - \partial_\mu B_\nu \quad . \end{aligned} \tag{18}$$

Coupled to the gauge fields is a complex scalar doublet

$$\Phi = \frac{1}{\sqrt{2}}\begin{pmatrix} \phi_1 + i\phi_2 \\ H + i\phi_0 \end{pmatrix} \quad , \tag{19}$$

with a scalar potential is given by

$$V(\Phi) = \mu^2 \mid \Phi^\dagger\Phi \mid + \lambda\Big(\mid \Phi^\dagger\Phi \mid\Big)^2 \quad , \tag{20}$$

($\lambda > 0$). This is the most general renormalizable and $SU(2)$ invariant potential allowed.

Just as in the Abelian model of Section 1.1, the state of minimum energy for $\mu^2 < 0$ is not at 0 and the scalar field develops a VEV. The direction of the minimum in $SU(2)_L$ space is not determined since the potential depends only on $\Phi^\dagger\Phi = \frac{1}{2}(\phi_1^2 + \phi_2^2 + H^2 + \phi_0^2)$ and we choose

$$\langle\Phi\rangle = \frac{1}{\sqrt{2}}\begin{pmatrix} 0 \\ v \end{pmatrix} \quad . \tag{21}$$

With this choice the scalar doublet has $U(1)_Y$ charge (hypercharge) $Y_\Phi = 1$ and the electromagnetic charge is $Q = T_3 + \frac{Y}{2}$. Therefore,

$$Q\langle\Phi\rangle = 0 \tag{22}$$

and electromagnetism is unbroken by the scalar VEV. The VEV of Eq. 21 hence yields the desired symmetry breaking scheme, $SU(2)_L \times U(1)_Y \rightarrow U(1)_{EM}$.

It is now straightforward to see how the Higgs mechanism generates mass for the W and Z gauge bosons. The contribution of the scalar fields to the Lagrangian is,

$$\mathcal{L}_s = (D^\mu\Phi)^\dagger(D_\mu\Phi) - V(\Phi) \tag{23}$$

where[3]

$$D_\mu = \partial_\mu + i\frac{g}{2}\tau \cdot W_\mu + i\frac{g'}{2}B_\mu. \tag{24}$$

In unitary gauge the scalar field can be written as

$$\Phi = \frac{1}{\sqrt{2}}\begin{pmatrix} 0 \\ v + H \end{pmatrix} \tag{25}$$

which gives the contribution to the gauge boson masses from the scalar kinetic energy term,

$$\frac{1}{2}(0 \quad v)\left(\frac{1}{2}g\tau \cdot W_\mu + \frac{1}{2}g'B_\mu\right)^2 \begin{pmatrix} 0 \\ v \end{pmatrix}. \tag{26}$$

Hence the gauge fields obtain a mass from the Higgs mechanism:

$$\begin{aligned} W_\mu^\pm &= \frac{1}{\sqrt{2}}(W_\mu^1 \mp iW_\mu^2) \\ Z^\mu &= \frac{-g'B_\mu + gW_\mu^3}{\sqrt{g^2 + g'^2}} \\ A^\mu &= \frac{gB_\mu + g'W_\mu^3}{\sqrt{g^2 + g'^2}}. \end{aligned} \tag{27}$$

The coupling constants satisfy the usual relations,

$$\begin{aligned} e &= g\sin\theta_W \\ e &= g'\cos\theta_W \end{aligned} \tag{28}$$

and the masses are given by

$$\begin{aligned} M_W^2 &= \frac{1}{4}g^2v^2 \\ M_Z^2 &= \frac{1}{4}(g^2 + g'^2)v^2 \\ M_\gamma &= 0. \end{aligned} \tag{29}$$

[3]The τ_i are the Pauli matrices with $Tr(\tau_i\tau_j) = 2\delta_{ij}$. Different choices for the gauge kinetic energy and the covariant derivative depend on whether g and g' are chosen positive or negative. There is no physical consequence of this choice.

It is again instructive to count the degrees of freedom after the spontaneous symmetry breaking has occurred. We began with a complex scalar field Φ with four degrees of freedom, a massless $SU(2)$ gauge field, W_i, with six degrees of freedom and a massless $U(1)$ gauge field, B, with 2 degrees of freedom for a total of 12. After the spontaneous symmetry breaking there remains a physical real scalar field H (1 degree of freedom), massive W and Z fields (9 degrees of freedom), and a massless photon (2 degrees of freedom). We say that the scalar degrees of freedom have been "eaten" to give the W and Z gauge bosons their longitudinal components.

Just as in the case of the Abelian Higgs model, if we go to a gauge other than unitary gauge, there will be Goldstone bosons in the spectrum and the scalar field can be written,

$$\Phi = \frac{e^{i\frac{\vec{\omega}\cdot\vec{\tau}}{v}}}{\sqrt{2}} \begin{pmatrix} 0 \\ v+H \end{pmatrix}. \tag{30}$$

In the Standard Model, there are three Goldstone bosons, $\vec{\omega} = (\omega^{\pm}, z)$, with masses M_W and M_Z in the Feynman gauge. These Goldstone bosons will play an important role in our understanding of the physics of a very heavy Higgs boson, $M_H > 1\ TeV$, as we will discuss in Section 5.1.

In addition to giving the W and Z bosons their masses, the Higgs boson is also used to give the fermions mass. The gauge invariant Yukawa coupling of the Higgs boson to fermions is

$$\mathcal{L}_f = -\lambda_d \overline{Q}_L \Phi d_R + h.c. \quad , \tag{31}$$

where the left handed $SU(2)$ fermion doublet is

$$Q_L = \begin{pmatrix} u \\ d \end{pmatrix}_L. \tag{32}$$

This gives the effective coupling

$$\lambda_d \frac{1}{\sqrt{2}} (\overline{u}_L,\ \overline{d}_L) \begin{pmatrix} 0 \\ v+H \end{pmatrix} d_R + h.c. \tag{33}$$

which can be seen to yield a mass term for the down quark if we make the identification

$$\lambda_d = \frac{m_d \sqrt{2}}{v}. \tag{34}$$

In order to generate a mass term for the up quark we use the fact that $\Phi^c \equiv -i\tau_2 \Phi^*$ is an $SU(2)$ doublet and we can write the $SU(2)$ invariant coupling

$$\lambda_u \overline{Q}_L \Phi^c u_R + h.c. \tag{35}$$

which generates a mass term for the up quark. Similar couplings can be used to generate mass terms for the charged leptons. For the multi-family case, the Yukawa couplings, λ_d and λ_u, become $N_F \times N_F$ matrices (where N_F is the number of families). Since the mass matrices and Yukawa matrices are proportional, the interactions of

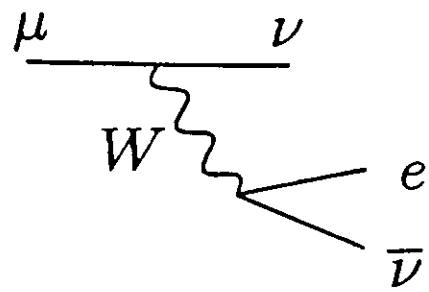

Figure 3: Determination of v from μ decay.

the Higgs boson with the fermion mass eigenstates are flavor diagonal. That is, the Higgs boson does not mediate flavor changing interactions.

By expressing the fermion kinetic energy in terms of the gauge boson mass eigenstates, the charged and neutral weak current interactions can be found. The parameter v can be determined from the charged current for μ decay, $\mu \to e\overline{\nu}_e\nu_\mu$, as shown in Fig. 3. Since the momentum carried by the W boson is of order m_μ it can be neglected in comparison with M_W and we make the identification

$$\frac{G_F}{\sqrt{2}} = \frac{g^2}{8M_W^2} = \frac{1}{2v^2}, \tag{36}$$

which gives the result $v^2 = (\sqrt{2}G_F)^{-1} = (246\ GeV)^2$.

One of the most important points about the Higgs mechanism is that all of the couplings of the Higgs boson to fermions and gauge bosons are completely determined in terms of coupling constants and fermion masses. The potential of Eq. 20 had two free parameters, μ and λ. We can trade these for

$$\begin{aligned} v^2 &= -\frac{\mu^2}{2\lambda} \\ M_H^2 &= 2v^2\lambda. \end{aligned} \tag{37}$$

There are no free adjustable parameters and so Higgs production and decay processes can be computed unambiguously in terms of the Higgs mass. In Fig. 4 we give a complete set of Feynman rules for the couplings of the Higgs boson. Note that for $M_H >> v$, the self couplings of the Higgs boson become strong.

2 Higgs Production in e^+e^- Colliders

Since the Higgs boson coupling to the electron is very small, $\sim m_e/v$, its dominant production mechanism in e^+e^- collisions is the so called "Bjorken Mechanism" shown in Fig. 5.[8] An estimate of the size of Higgs production can be found from the decay

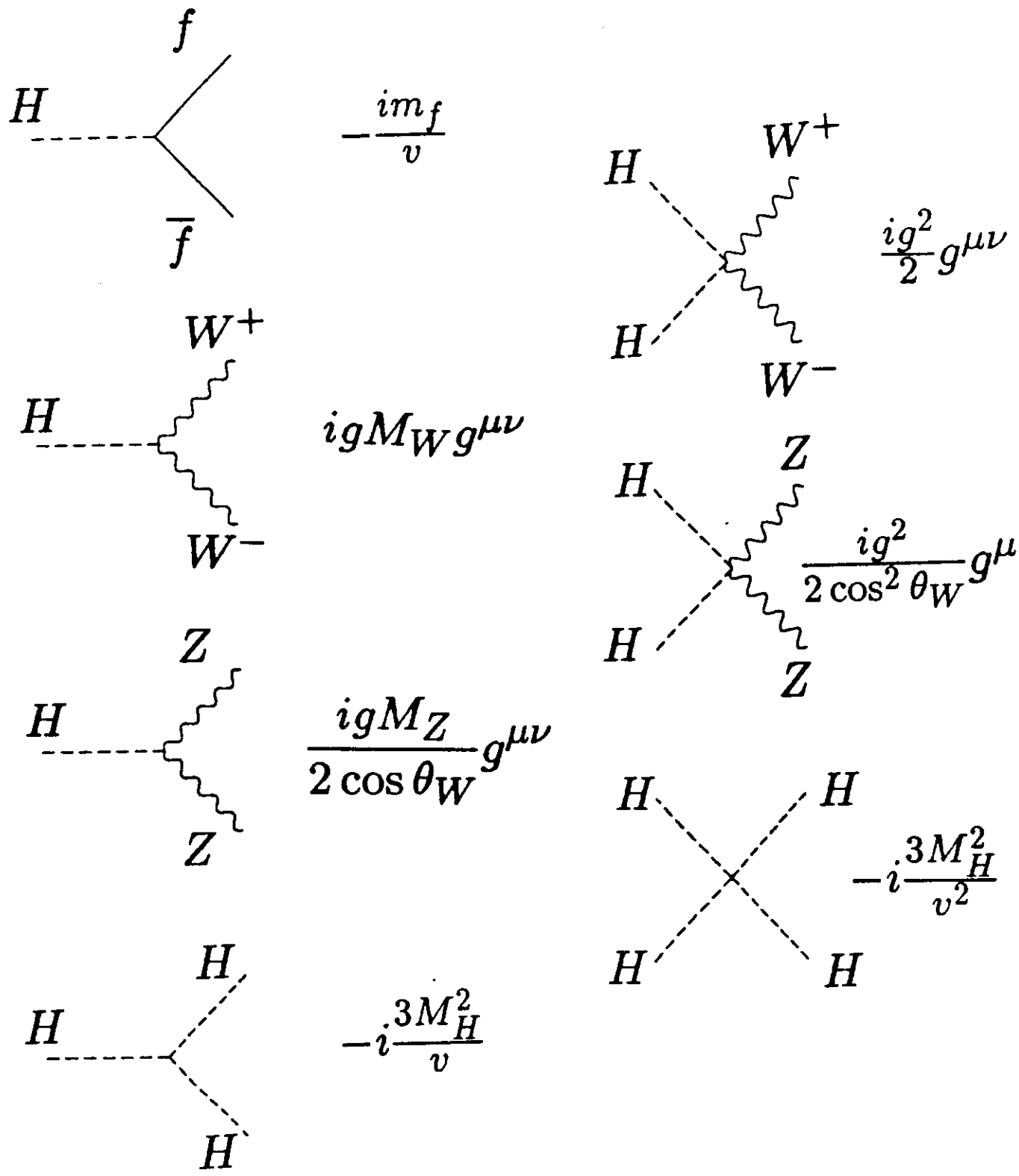

Figure 4: Feynman rules for the Standard Model Higgs boson.

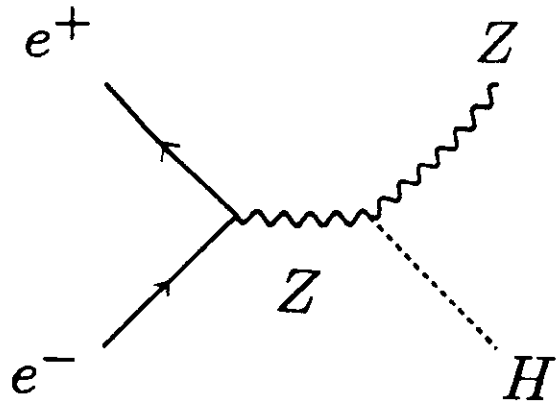

Figure 5: Higgs production through $e^+e^- \to ZH$.

$Z \to Hf\bar{f}$ for a massless Higgs boson:

$$\frac{BR(Z \to Hf\bar{f})}{BR(Z \to f\bar{f})}\,|_{M_H=0} = \frac{g^2}{192\pi^2 \cos\theta_W^2}\left[\left(6 - \frac{\Gamma_Z^2}{2M_Z^2}\right)\log\left(\frac{\Gamma_Z^2 + M_Z^2}{\Gamma_Z^2}\right) + \frac{12\Gamma_Z}{M_Z}\tan^{-1}\left(\frac{M_Z}{\Gamma_Z}\right) - \frac{23}{2}\right] \sim 10^{-2}, \tag{38}$$

where Γ_Z is the total Z boson decay width. We can see from Eq. 38 that Higgs boson production in Z decays can never be more than a few percent effect.

The Higgs boson has been searched for in e^+e^- collisions at the LEP collider, which has $\sqrt{s} = M_Z$. The Higgs is produced through the mechanism of Fig. 5, but with the final Z off-shell and decaying to a lepton pair. The primary decay mechanism used is $Z \to Hl^+l^-$ whose branching ratio is shown in Fig. 6. The decay $Z \to H\nu\bar{\nu}$ is also useful since the branching ratio is 6 times larger than that of $Z \to He^+e^-$. The strategy is to search for each range of Higgs mass separately by looking for the relevant Higgs decays. For example, a light Higgs boson, $M_H < 2m_e$, necessarily decays to 2 photons. For $M_H \sim 1\ MeV$, the Higgs lifetime gives $c\tau \sim 10^3\ cm$ and so the Higgs boson is long lived and escapes the detector without interacting. In this case the relevant reaction is $e^+e^- \to Z \to l^+l^-H$ and the signal is l^+l^- plus missing energy from the undetected Higgs boson. For each mass region, the appropriate Higgs decay channels are searched for. When the Higgs becomes heavier than twice the b quark mass it decays primarily to $b\bar{b}$ pairs and the signal is then $e^+e^- \to Z \to l^+l^-H \to l^+l^-$ + jets. By a systematic study of all Higgs boson masses and decay channels, the LEP experiments have found the limit[9][4]

$$M_H > 58\ GeV. \tag{39}$$

[4]Note that there is no region where light Higgs boson masses are allowed. The LEP limits thus obviate early studies of mechanisms such as $K \to \pi H$ or $B \to \pi H$.

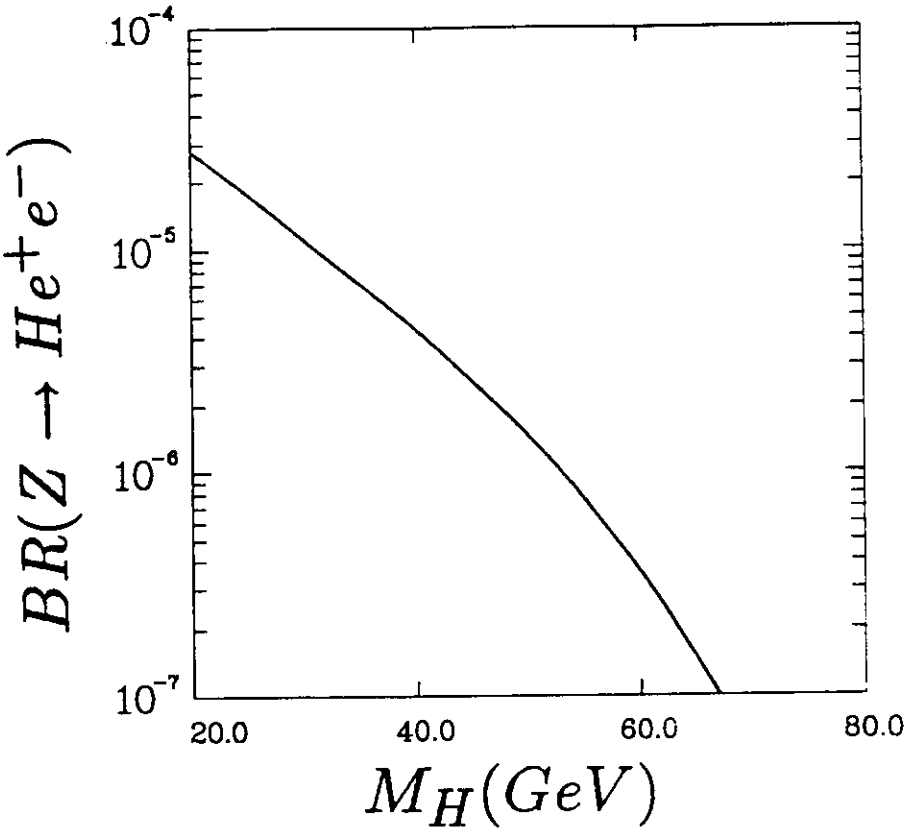

Figure 6: Branching ratio for $Z \to He^+e^-$.

Since the LEP experiments have on the order of one million Z's we see from Fig. 6 that the number of Higgs events expected for higher masses is quite small and this limit is not expected to be significantly improved by future running.[10]

In the future, LEPII will run at an energy somewhere above $\sqrt{s} \sim 175\ GeV$ and so will look for the process $e^+e^- \to ZH$ shown in Fig. 5. The only difference between this process and the searches at LEP is that now the final state Z can be on-shell. The cross section for this process at a center- of- mass energy s is,[11]

$$\sigma(e^+e^- \to HZ) = \frac{\pi\alpha^2\sqrt{\lambda}(\lambda + 12sM_Z^2)[1 + (1 - 4\sin^2\theta_W)^2]}{192s^2\sin^4\theta_W\cos^4\theta_W(s - M_Z^2)^2} \tag{40}$$

where $\lambda \equiv (s - M_H^2 - M_Z^2)^2 - 4M_H^2M_Z^2$. (In the center of mass, the momentum of the outgoing Z is $\frac{\sqrt{\lambda}}{2\sqrt{s}}$). From this we can see that the cross section peaks at an energy $\sqrt{s} \sim M_Z + \sqrt{2}M_H$. This is a very clean production channel with little background and LEPII is expected to be able to explore the Higgs mass region up to the kinematic limit, $M_H < \sqrt{s} - M_Z \sim \mathcal{O}(80\ GeV)$.

In Fig. 7, we show the total cross section for $e^+e^- \to ZH$ as a function of $\sqrt{s}$ for fixed M_H. If we demand 40 ZH events with $Z \to e^+e^- + \mu^+\mu^-$ in 1000 pb^{-1} to discover the Higgs in this channel, then we require $\sigma > .7\ pb$ which implies that LEPII will be sensitive to $M_H < 80\ GeV$, which is consistent with our estimate that LEPII will reach the kinematic limit.

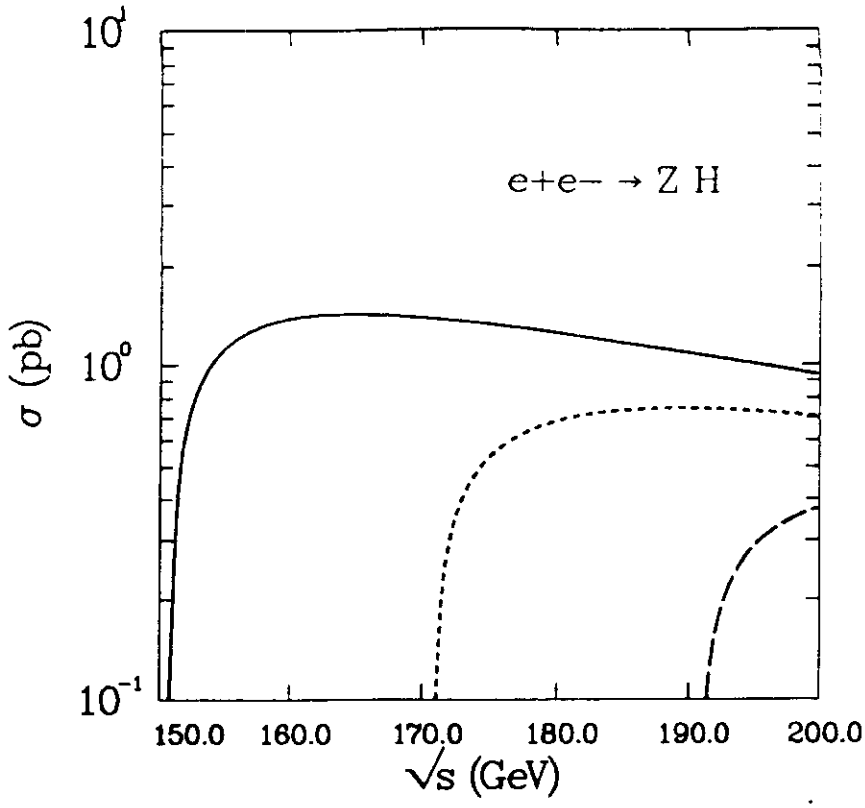

Figure 7: Total cross section for $e^+e^- \to ZH$. The solid, dotted, and dashed lines have $M_H = 60$, 80 and 100 GeV, respectively.

3 Higgs Production in Hadronic Collisions

3.1 Gluon Fusion

We turn now to the production of the Higgs boson in pp or $p\bar{p}$ collisions. Since the coupling of a Higgs boson to an up quark or a down quark is proportional to the quark mass, this coupling is very small. The primary production mechanism for a Higgs boson in hadronic collisions is through gluon fusion, $gg \to H$, which is shown in Fig. 8. The loop contains all quarks with mass m. (In extensions of the standard model, all massive colored particles run in the loop.) To evaluate the diagram of Fig. 8, we use dimensional regularization in $n = 4 - 2\epsilon$ dimensions. For a fermion of mass m in the loop the amplitude given by the diagram of Fig. 8. is

$$i\mathcal{A} = -(-ig_s)^2 Tr(T_A T_B)\left(\frac{-im}{v}\right)\int \frac{d^n k}{(2\pi)^n}\frac{T^{\mu\nu}}{D}(i)^3 \epsilon_\mu(p)\epsilon_\nu(q) \qquad (41)$$

where the overall minus sign is due to the closed fermion loop.[5] The denominator is $D = (k^2 - m^2)[(k+p)^2 - m^2][(k-q)^2 - m^2]$. The usual method of Feynman parameterization can be used to combine the denominators,

$$\frac{1}{ABC} = 2\int_0^1 dx \int_0^{1-x} \frac{dy}{[Ax + By + C(1-x-y)]^3} \qquad (42)$$

[5] $\epsilon_\mu(p)$ are the transverse gluon polarizations.

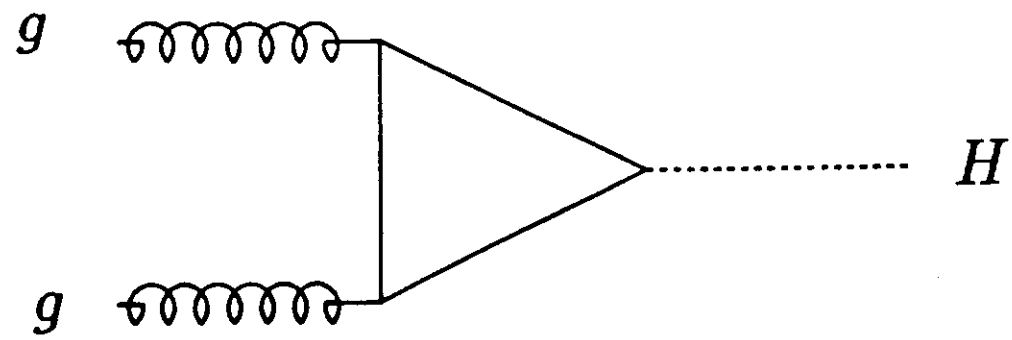

Figure 8: Higgs boson production through gluon fusion with a quark loop.

and so the denominator becomes,

$$\frac{1}{D} \to 2\int dx\, dy \frac{1}{[k^2 - m^2 + 2k\cdot(px - qy)]^3}. \tag{43}$$

Shifting the integration momenta, $k' = k + px - qy$, the denominator takes the form

$$\frac{1}{D} \to 2\int dx\, dy \frac{1}{[k'^2 - m^2 + M_H^2 xy]^3}. \tag{44}$$

The numerator of Eq. 41 is also easily evaluated

$$\begin{aligned} T^{\mu\nu} &= Tr\Big[(k+m)\gamma^\mu(k+p+m)(k-q+m)\gamma^\nu)\Big] \\ &= 4m\Big[g^{\mu\nu}(m^2 - k^2 - \frac{M_H^2}{2}) + 4k^\mu k^\nu + p^\nu q^\mu\Big] \end{aligned} \tag{45}$$

where we have used the fact that for transverse gluons, $\epsilon(p)\cdot p = 0$ and so terms proportional to p_μ or q_ν can be dropped. We now shift momenta, drop terms linear in k' from the numerator and use the relation

$$\int d^n k' \frac{k'^\mu k'^\nu}{(k'^2 - C)^m} = \frac{1}{n} g^{\mu\nu} \int d^n k' \frac{k'^2}{(k'^2 - C)^m} \tag{46}$$

to write the amplitude in the form

$$\begin{aligned} i\mathcal{A} &= -\frac{2g_s^2 m^2}{v}\delta_{AB}\int \frac{d^n k'}{(2\pi)^n}\int dx dy \Big\{ g^{\mu\nu}\Big[m^2 + k'^2\Big(\frac{4}{n} - 1\Big) + M_H^2(xy - \frac{1}{2})\Big] \\ &\quad + p^\nu q^\mu(1 - 4xy)\Big\}\frac{2dxdy}{(k'^2 - m^2 + M_H^2 xy)^3}\epsilon_\mu(p)\epsilon_\nu(q). \end{aligned} \tag{47}$$

The integral of Eq. 47 can easily be done using the well known formulas of dimensional regularization[12]

$$\begin{aligned}\int \frac{d^n k'}{(2\pi)^n} \frac{k'^2}{(k'^2 - C)^3} &= \frac{i}{32\pi^2}(4\pi)^\epsilon \frac{\Gamma(1+\epsilon)}{\epsilon}(2-\epsilon)C^{-\epsilon} \\ \int \frac{d^n k}{(2\pi)^n} \frac{1}{(k'^2 - C)^3} &= -\frac{i}{32\pi^2}(4\pi)^\epsilon \Gamma(1+\epsilon)C^{-1-\epsilon}. \end{aligned} \tag{48}$$

We find the well known result[13]

$$\mathcal{A}(gg \to H) = -\frac{\alpha_s m^2}{\pi v}\delta_{AB}\Big(g^{\mu\nu}\frac{M_H^2}{2} - p^\nu q^\mu\Big)\int dxdy\Big(\frac{1-4xy}{m^2 - M_H^2 xy}\Big)\epsilon_\mu(p)\epsilon_\nu(q). \tag{49}$$

(Note that we have multiplied by 2 in Eq. 49 to include the diagram where the gluon legs are crossed.) The Feynman integral of Eq. 49 can easily be performed to find an analytic result if desired.

It is particularly interesting to consider the case when the fermion in the loop is much more massive than the Higgs boson, $m >> M_H$. In this case we find,

$$\mathcal{A}(gg \to H) \longrightarrow_{m>>M_H} -\frac{\alpha_s}{3\pi v}\delta_{AB}\Big(g^{\mu\nu}\frac{M_H^2}{2} - p^\nu q^\mu\Big)\epsilon_\mu(p)\epsilon_\nu(q). \tag{50}$$

We see that the production process $gg \to H$ is independent of the mass of the heavy fermion in the loop in the limit $m >> M_H$. Hence it counts the number of heavy generations and is a window into new physics at scales much above the energy being probed. This is a contradiction of our intuition that heavy particles should decouple and not affect the physics at lower energy. The reason the heavy fermions do not decouple is, of course, because the Higgs boson couples to the fermion mass.[15]

Resonant production of a heavy Higgs can be found from the standard formula:[14]

$$\hat{\sigma}(gg \to H) = \frac{\pi^2}{8M_H^3}\Gamma(H \to gg)\delta(1 - \frac{M_H^2}{\hat{s}}). \tag{51}$$

It is straightforward to obtain our parton level result:

$$\hat{\sigma}(gg \to H) = \frac{\alpha_s^2}{64\pi v^2}M_H^2 \mid I\Big(\frac{M_H^2}{m^2}\Big) \mid^2 \delta(\hat{s} - M_H^2) \tag{52}$$

where $\sqrt{\hat{s}}$ is the energy in the gluon -gluon center of mass and the integral I is defined by

$$I(a) \equiv \int_0^1 dx \int_0^{1-x} dy \frac{1-4xy}{1-axy}. \tag{53}$$

In Fig. 9 we plot $I(a)$ and see that it goes quickly to its large a value. Numerically, the heavy fermion mass limit is an extremely good approximation even for $m \sim M_H$. From this plot we can also see that the contribution of light quarks to gluon fusion of the Higgs boson is irrelevant. In fact we have,

$$I(a) \longrightarrow_{a\to\infty} \sim -\frac{1}{2a}\log^2(a). \tag{54}$$

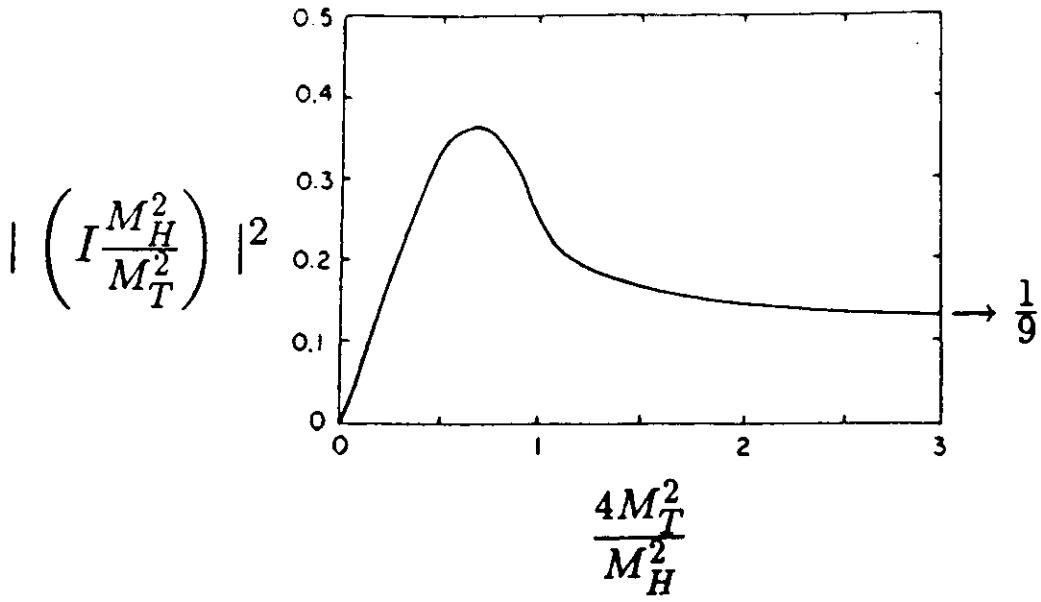

Figure 9: Form factor for gluon fusion, $|\, I\left(\frac{4M_T^2}{M_H^2}\right)|^2$.

Therefore, for the Standard Model, only the top quark is numerically important when computing Higgs boson production from gluon fusion.

To find the physical cross section we must integrate with the distribution of gluons in a proton,[22]

$$\sigma(pp \rightarrow H) = \int dx_1 dx_2 g(x_1) g(x_2) \hat{\sigma}(gg \rightarrow H), \tag{55}$$

where $g(x)$ is the distribution of gluons in the proton. Better numerical convergence is obtained if we make the transformation of variables, $x_1 \equiv \sqrt{\tau} e^y$, $x_2 \equiv \sqrt{\tau} e^{-y}$, and $\tau \equiv M_H^2/\hat{s}$. The result is then,

$$\sigma(pp \rightarrow H) = \frac{\alpha_s^2}{64\pi v^2} M_H^2 \,|\, I\left(\frac{M_H^2}{m^2}\right)|^2 \, \frac{1}{s}\frac{d\mathcal{L}}{d\tau} \tag{56}$$

where the gluon- gluon luminosity is defined

$$\frac{\tau}{s}\frac{d\mathcal{L}}{d\tau} \equiv \frac{1}{s}\int_{\log(\sqrt{\tau})}^{-\log(\sqrt{\tau})} dy \; g\left(\sqrt{\tau}e^y\right) g\left(\sqrt{\tau}e^{-y}\right). \tag{57}$$

The gluon-gluon luminosity is shown in Fig. 10 for Tevatron and LHC energies. We see that the luminosity increases rapidly with energy.

It is straightforward to use the results given above to find the cross section for Higgs production at the LHC (Large Hadron Collider), a planned pp collider at CERN with an energy of 14 TeV. We show in Fig. 11 the cross section for producing a Higgs boson at the LHC. The resonant structure in the figure occurs at $M_H \sim 2M_T$ and is due to the fact that the amplitude for $gg \rightarrow H$ gets an imaginary part for $M_H > 2M_T$,

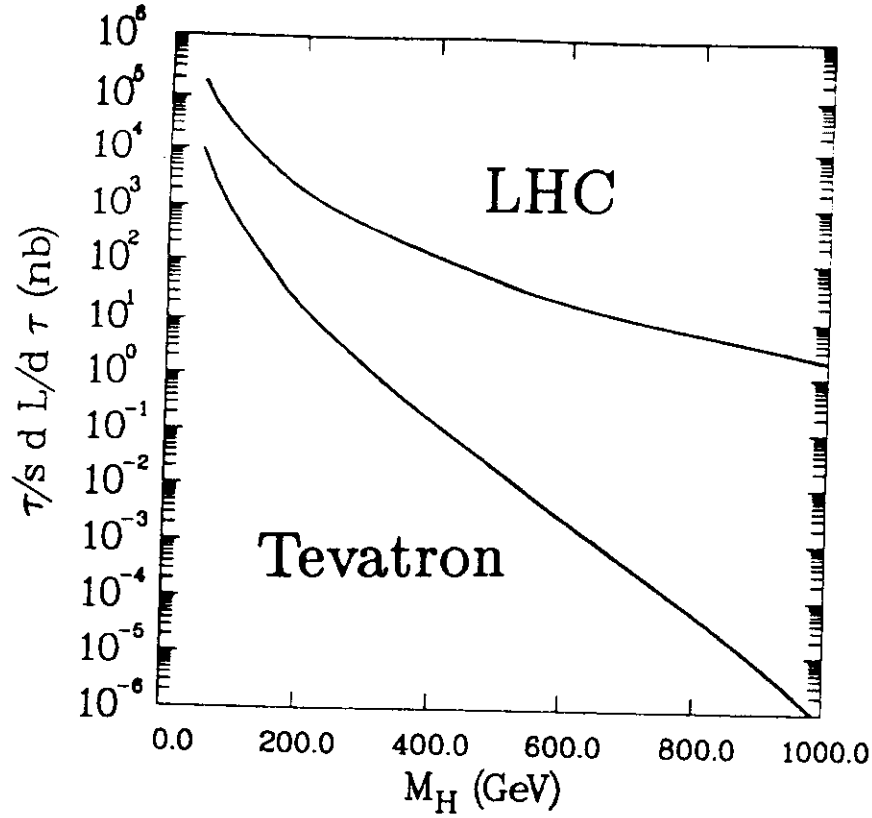

Figure 10: Gluon-gluon luminosity in pp (or $p\bar{p}$) collisions at $\sqrt{s} = 1.8\ TeV$ and $14\ TeV$. The gluon-gluon center- of- mass energy, $\sqrt{\hat{s}}$, is equal to M_H for Higgs production.

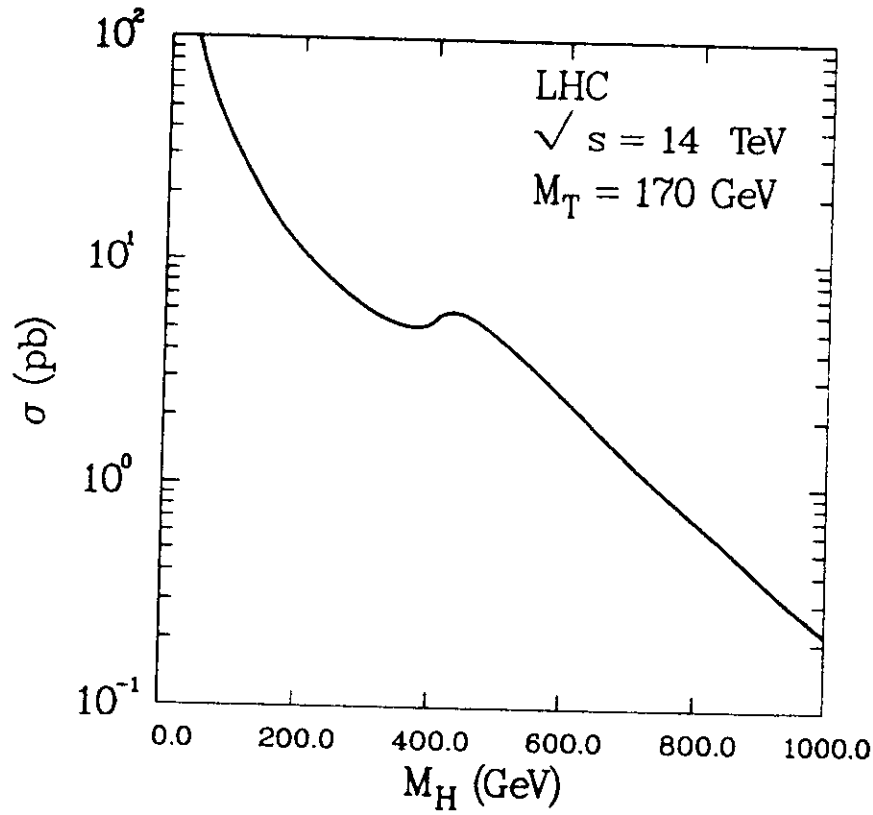

Figure 11: Cross section for Higgs production from gluon fusion at the LHC from a top quark with $M_T = 170\ GeV$.

as can be seen from the integral of Eq. 53. The planned luminosity at the LHC is $\mathcal{L} = 10^{34}/cm^2/sec$. Hence a cross section of 1 pb corresponds to roughly 10^5 events per year, (a theorists year is typically taken to be $10^7 sec/year$). In Section 3.3 we will investigate whether these 10^5 events are actually observable.

3.2 Low Energy Theorem

A striking feature of our result for Higgs boson production from gluon fusion is that it is independent of the heavy quark mass for a light Higgs boson. In fact Eq. 50 can be derived from the effective vertex,[16, 23, 25]

$$\begin{aligned} \mathcal{L}_{\text{eff}} &= \frac{\alpha_s}{12\pi} G^A_{\mu\nu} G^{A\ \mu\nu} \left(\frac{H}{v}\right) \\ &= \frac{\beta_F}{g_s} G^A_{\mu\nu} G^{A\ \mu\nu} \left(\frac{H}{2v}\right)(1-\delta), \end{aligned}$$

where

$$\beta_F = \frac{g_s^3 N_H}{24\pi^2} \tag{58}$$

is the contribution of heavy fermion loops to the $SU(3)$ beta function and $\delta = 2\alpha_s/\pi$.[6] (N_H is the number of heavy fermions with $m >> M_H$.) The effective Lagrangian of Eq. 58 gives ggH and $gggH$ vertices and can be used to compute the radiative corrections of $\mathcal{O}(\alpha_s^3)$ to gluon production.[16] The correction in principle involve 2-loop diagrams. However, using the effective vertices from Eq. 58, the $\mathcal{O}(\alpha_s^3)$ corrections can be found from a 1-loop calculation.

In Fig.13 we show the radiatively corrected result for Higgs production from gluon fusion. Several important facts can be seen from this figure. The first is that there is very little dependance on the top quark mass and hence the heavy fermion mass limit (where all terms of $\mathcal{O}(M_H^2/M_T^2)$ are neglected) is quite accurate. When computing the lowest order result from the triangle diagram of Fig. 8, such as that shown in Fig. 11, it is ambiguous whether to use the one or two loop equation for α_s and which structure functions to use, a set fit to data using only the lowest order (in α_s) predictions or a set which includes some higher order effects.[26] The difference between the equations for α_s and the different structure functions is $\mathcal{O}(\alpha_s^2)$ and hence higher order in α_s when one is computing the "lowest order" result. In Fig.13 we show 2 different definitions of the lowest order result and see that they differ significantly from each other. It is interesting that the consistent $\mathcal{O}(\alpha_s^2)$ result (that with one loop α_s and lowest order structure functions) is closest to the radiatively corrected result. We see that the radiative corrections are large and increase the production rate by about a factor of 1.5 from the lowest order result.

[6] The $(1-\delta)$ term arises from a subtlety in the use of the low energy theorem. Since the Higgs coupling to the heavy fermions is $M_f(1+\frac{H}{v})\overline{f}f$, the counterterm for the Higgs Yukawa coupling is fixed in terms of the renormalization of the fermion mass and wavefunction. The beta function, on the other hand, is evaluated at $q^2 = 0$. The $1-\delta$ term corrects for this mismatch.[24]

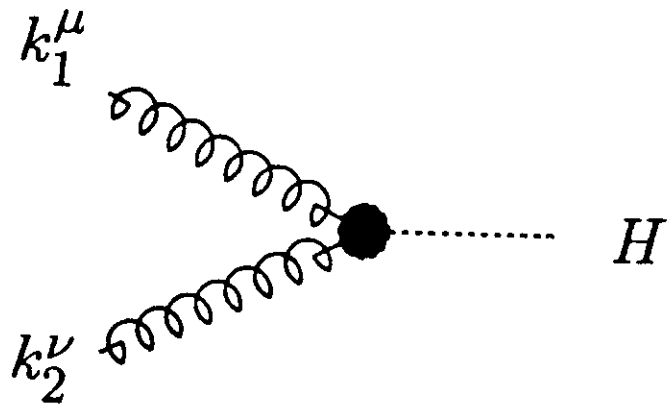

$$\frac{\alpha_s}{3\pi v}\left(g^{\mu\nu}k_1\cdot k_2 - k_1^\nu k_2^\mu\right)$$

Figure 12: Effective ggH vertex.

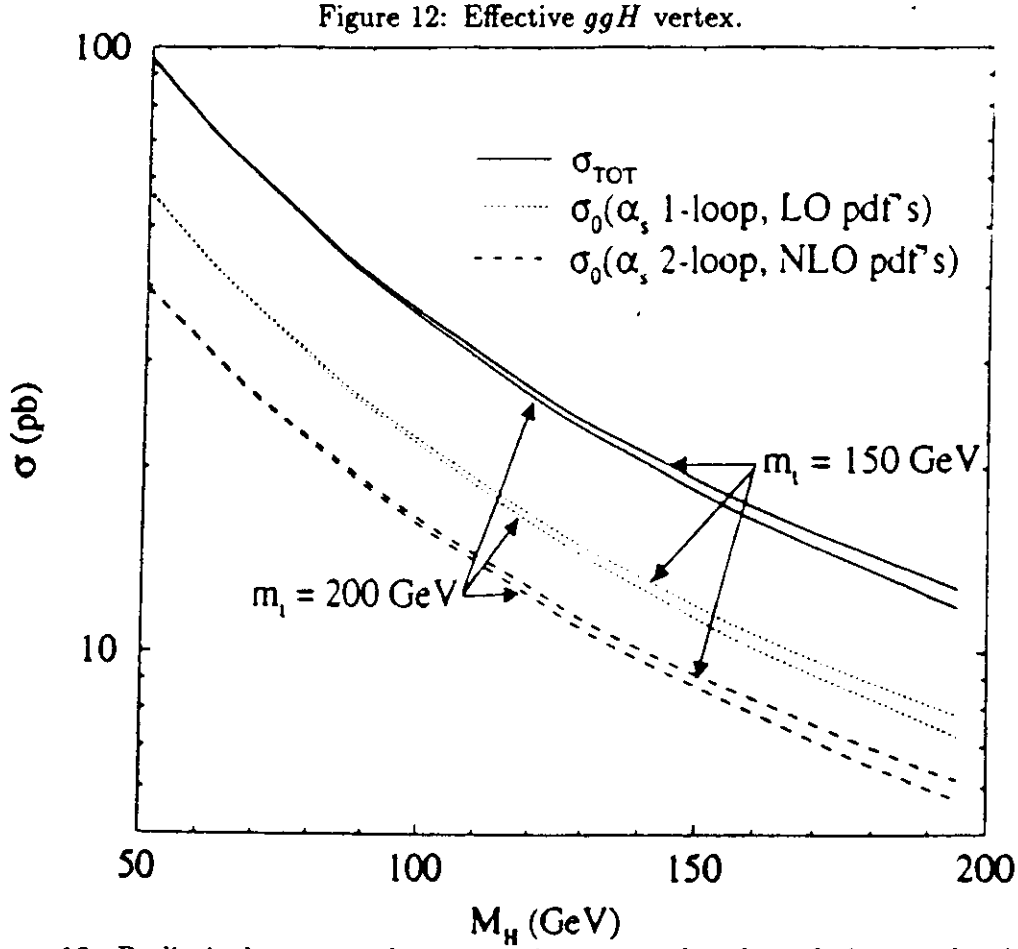

Figure 13: Radiatively corrected cross section, $\sigma_{\rm TOT}$, for gluon fusion production of the Higgs boson at the LHC.

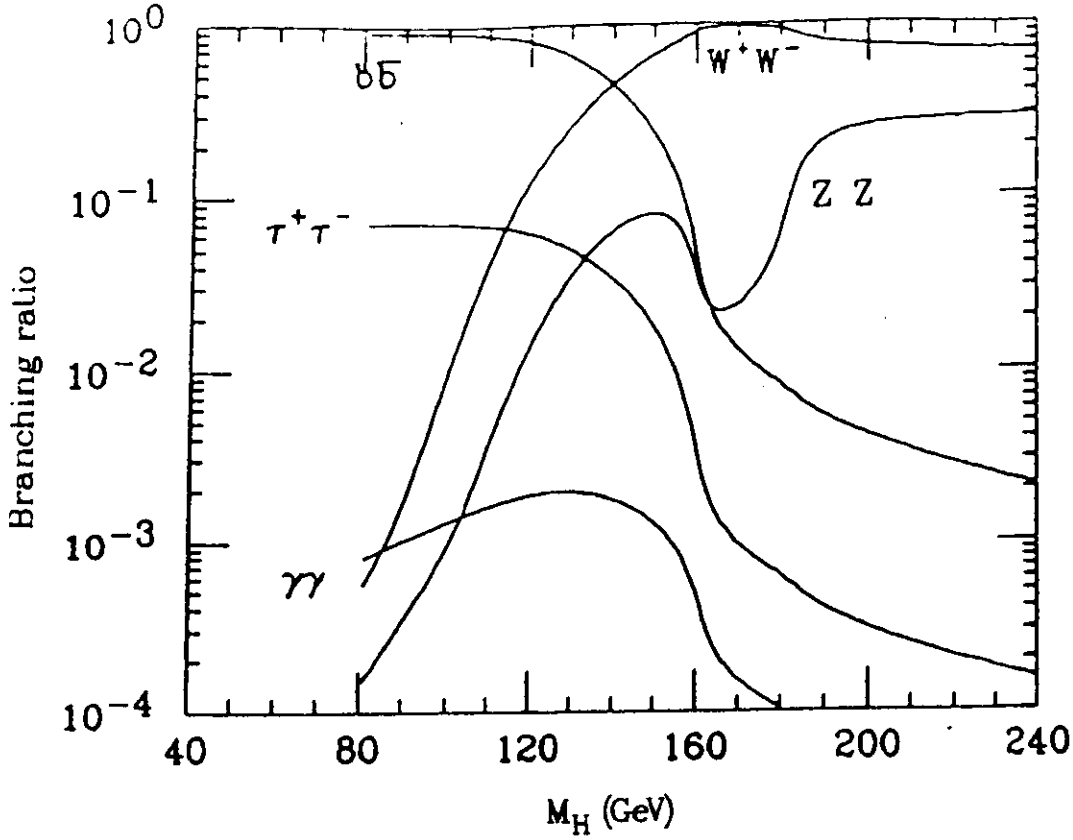

Figure 14: Branching ratios for the intermediate mass Higgs boson.

3.3 Finding the Higgs Boson at the LHC

We turn now to a discussion of search techniques for the Higgs boson at the LHC. For $M_H < 800\ GeV$, gluon fusion is the primary production mechanism, (for $M_T \sim 170\ GeV$). At the present time, there are two large detectors planned for the LHC; the ATLAS detector[18] and the CMS detector[19]. We will present several results from preliminary studies of these collaborations on the capabilities of the LHC to discover the Higgs boson in various decay channels. Detailed discussions of the experimental problems involved can be found in the collaborations reports.

We have seen that the production rate for the Higgs boson at the LHC is significant, $\sigma_H \sim .1 - 10\ pb$ for $200\ GeV < M_H < 1\ TeV$. However, in order to see the Higgs boson it must decay into some channel where it is not overwhelmed by the background. For $M_H < 2M_W$ the Higgs boson decays predominantly to $b\bar{b}$ pairs, (remember that the Higgs coupling to fermions is proportional to the fermion mass). Unfortunately, the QCD production of b quarks is many orders of magnitude larger than Higgs production and so this channel is thought to be useless.[17] One is led to consider rare decay modes of the Higgs boson where the background may be smaller. The decay channels which have received the most attention are $H \to \gamma\gamma$ and $H \to ZZ^*$.[20][7] The branching ratios for these decays are shown in Fig. 14 and can be

[7]References to the many studies of the decays $H \to \gamma\gamma$ and $H \to ZZ^*$ can be found in Refs. [18, 19].

seen to be quite small. (The rate for off-shell gauge bosons, $H \to VV^*$, $(V = W^{\pm}, Z)$ must be multiplied by the relevant branching ratio, $V \to f'\bar{f}$.)

The $H \to ZZ^*$ decay mode can lead to a final state with 4 leptons, 2 of whose mass reconstructs to M_Z while the invariant mass of the 4 lepton system reconstructs to M_H. The largest background to this decay is $t\bar{t}$ production with $t \to Wb \to (l\nu)(cl\nu)$. There are also backgrounds from $Zb\bar{b}$ production, ZZ^* production, etc. For $M_H = 150\ GeV$, the ATLAS collaboration estimates that there will be 184 signal events and 840 background events in their detector in one year from $H \to ZZ^* \to (4l)$ with the 4-lepton invariant mass in a mass bin within $\pm 2\sigma$ of M_H.[18] The leptons from Higgs decay tend to be more isolated from other particles than those coming from the backgrounds and a series of isolation cuts can be used to reduce the rate to 92 signal and 38 background events. The ATLAS collaboration claims that they will be able to discover the Higgs boson in the $H \to ZZ^* \to l^+l^-l^+l^-$ mode for $130\ GeV < M_H < 180\ GeV$ with an integrated luminosity of $10^5 pb^{-1}$ (one year of running at the LHC at design luminosity) and using both the electron and muon signatures. For $M_H < 130\ GeV$, there are not enough events since the branching ratio is too small (see Fig. 14), while for $M_H > 180\ GeV$ the Higgs search will proceed via the $H \to ZZ$ channel, which we discuss in Section 4.3.

For $M_H < 130\ GeV$, the Higgs boson can be searched for through its decay to 2 photons. The branching ratio in this region is about 10^{-3}, so for a Higgs boson with $M_H \sim 100\ GeV$ there will be about 3000 events per year, ($\sigma \sim 30\ pb$ and the LHC design luminosity is $10^{34}/cm^2/sec$.) The Higgs boson decay into the $\gamma\gamma$ channel is an extremely narrow resonance in this region with a width around 1 KeV. From Fig. 14 we see that the branching ratio for $H \to \gamma\gamma$ falls off rapidly with increasing M_H and so this decay mode is probably only useful in the region $80\ GeV < M_H < 130\ GeV$.[8]

The irreducible background to $H \to \gamma\gamma$ comes from $q\bar{q} \to \gamma\gamma$ and $gg \to \gamma\gamma$ and is shown in Fig. 15. In Fig. 16 we show the signal and the background for a Higgs boson of mass $M_H = 110\ GeV$ at the LHC using the ATLAS detector. Extracting such a narrow signal from the immense background poses a formidable experimental challenge. The detector must have a mass resolution on the order of $\delta m/m \sim 1.5\%$ in order to be able to hope to observe this signal. For $M_H = 110\ GeV$ there are 1430 signal events and 25,000 background events in a mass bin equal to the Higgs width. This leads to a ratio ,

$$\frac{\text{Signal}}{\sqrt{\text{Background}}} \sim 9. \tag{59}$$

A ratio greater than 5 is usually *defined* as a discovery. ATLAS claims that they will be able to discover the Higgs boson in this channel for $100\ GeV < M_H < 130\ GeV$. (Below 100 GeV the background is too large and above 130 GeV the event rate is too small.)

There are many additional difficult experimental problems associated with the

[8]The $H \to \gamma\gamma$ branching ratio is sensitive to the top quark mass. However, unlike the case $gg \to H$, there are Feynman diagrams with W bosons in the loop which dominate over the top quark contribution.

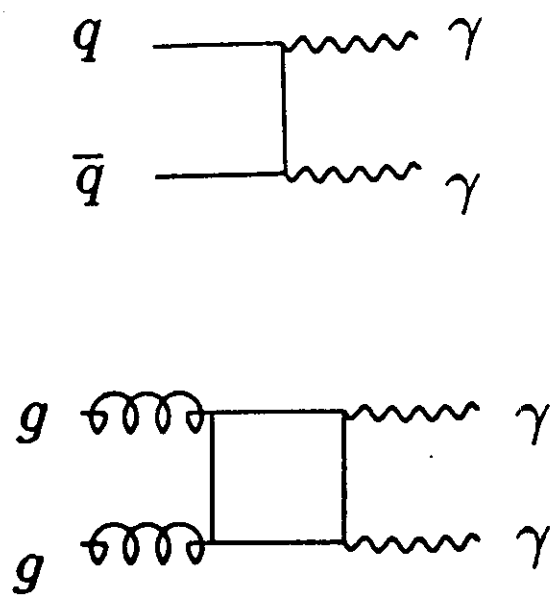

Figure 15: Irreducible backgrounds to $H \to \gamma\gamma$; $q\bar{q} \to \gamma\gamma$ and $gg \to \gamma\gamma$.

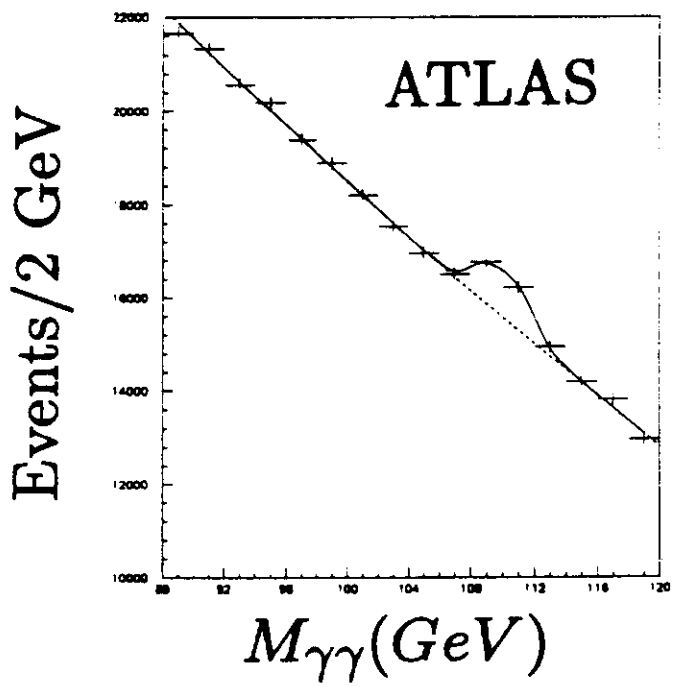

Figure 16: Expected $M_{\gamma\gamma}$ signal for $H \to \gamma\gamma$ signal above the irreducible $\gamma\gamma$ background for $M_H = 110\ GeV$ at the LHC using the ATLAS detector. This figure is from Ref. [18].

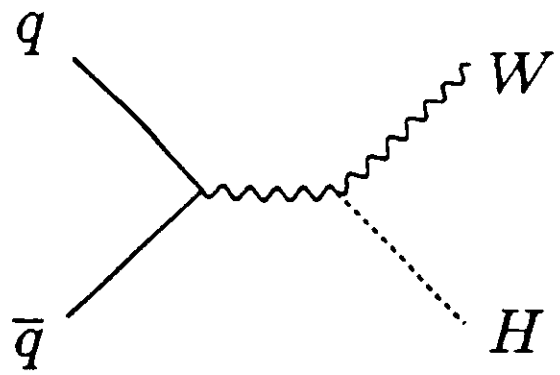

Figure 17: Production of the Higgs boson through $q\bar{q} \rightarrow WH$.

decay channel $H \rightarrow \gamma\gamma$. The most significant of these is the confusion of a photon with a jet. Since the cross section for producing jets is so much larger than that of $H \rightarrow \gamma\gamma$ the experiment must not mistake a photon for a jet more than one time in 10^4. It has not yet been demonstrated that this is experimentally feasible.

One might think that the decay $H \rightarrow \tau^+\tau^-$ would be useful since as shown in Fig. 14 its branching ratio is considerably larger than $H \rightarrow ZZ^*$ and $H \rightarrow \gamma\gamma$, $BR(H \rightarrow \tau^+\tau^-) \sim 3.5\%$ for $M_H = 110\ GeV$. The problem is that for the dominant production mechanism, $gg \rightarrow H$, the Higgs boson has no transverse momentum and so the $\tau^+\tau^-$ invariant mass cannot be reconstructed. If we use the production mechanism, $gg \rightarrow Hg$, then the Higgs is produced at large transverse momentum and it is possible to reconstruct the $\tau\tau$ invariant mass. Unfortunately, however, the background from $q\bar{q} \rightarrow \tau^+\tau^-$ and from $t\bar{t}$ decays overwhelms the signal.[23]

3.4 Higgs Boson Production at the Tevatron

Since it will be some years before the LHC comes into operation it is worth considering whether any relevant limits on the Higgs boson can be obtained from the existing hadron collider, the Tevatron, which is a $p\bar{p}$ collider with an energy $\sqrt{s} = 1.8\ TeV$. For a Higgs boson mass of 60 GeV the production cross section at the Tevatron is roughly 4 pb. At a luminosity of $\mathcal{L} \sim 10^{31}/cm^2/sec$ this yields 400 Higgs events per year. To look at these events in the $\gamma\gamma$ decay mode we must multiply by a branching ratio of 10^{-3} which leaves .4 Higgs events per year. Even with the main injector, which will increase the luminosity by about a factor of 10, finding the Higgs boson through this decay channel is clearly hopeless at the Tevatron.

Recently it has been suggested that it may be fruitful to look for the Higgs boson at the Tevatron through the production mechanism $q\bar{q} \rightarrow WH$, shown in Fig. 17.[27, 28] The various production mechanisms which are relevant for producing a Higgs boson at the Tevatron are shown in Fig. 18. The cross section for $q\bar{q} \rightarrow WH$ is about 1 pb

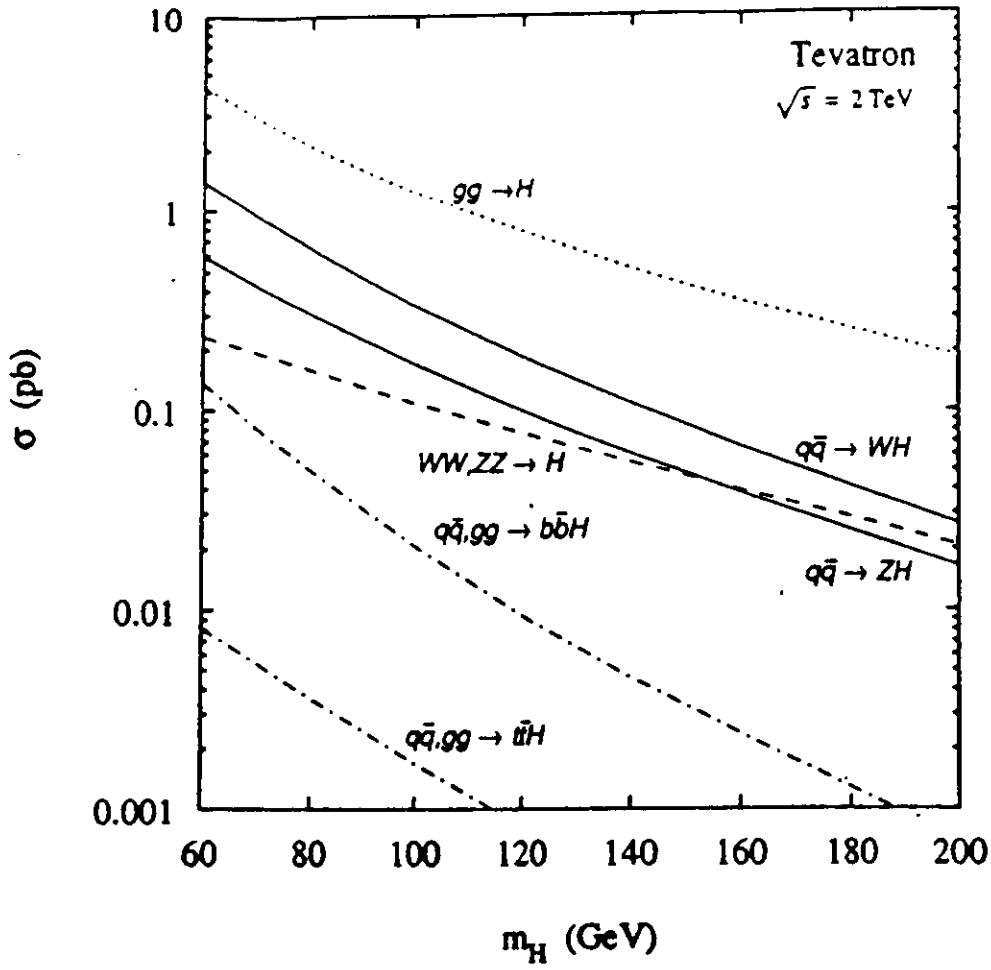

Figure 18: Higgs boson production at the Tevatron.

which gives on the order of 20 events/year if we look at the decays $W \to e\bar{\nu}$ and $W \to \mu\bar{\nu}$. Unfortunately, the cuts to eliminate backgrounds make this mechanism not viable. Potential upgrades to increase either the luminosity or the energy at the Tevatron may make this a viable option.[27, 28] The WH production mechanism may also be useful at the LHC to look for a Higgs boson in the $M_H \sim 100\ GeV$ region.

4 Higgs Boson Production from Vector Bosons

4.1 The Effective W Approximation

We turn now to the study of the couplings of the Higgs bosons to gauge bosons. We begin by studying the diagram in Fig. 19. Naively, one expects this diagram to give a negligible contribution to Higgs production because of the two W boson propagators. However, it turns out that this production mechanism can give an important contribution. The diagram of Fig. 19 can be interpreted in parton model language as the resonant scattering of two W bosons to form a Higgs boson[31] and we can compute the distribution of W bosons in a quark in an analogous manner to the computation of the distribution of photons in an electron.[30] By considering the W and Z gauge bosons as partons, calculations involving gauge bosons in the intermediate states can be considerably simplified.

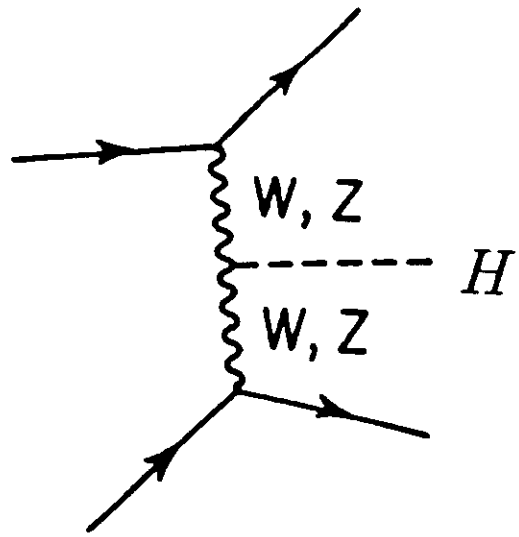

Figure 19: Higgs boson production from WW fusion.

We define orthogonal polarization tensors for a W boson with momentum $k = (k_0, 0, 0, |\vec{k}|)$:

$$\begin{aligned} \text{Transverse}: \quad \epsilon_\pm &= \frac{1}{\sqrt{2}}(0, 1, \pm i, 0) \\ \text{Longitudinal}: \quad \epsilon_L &= \frac{1}{M_W}(|\vec{k}|, 0, 0, k_0). \end{aligned} \tag{60}$$

For large momentum, $k_0 >> M_W$, we have

$$\epsilon_L \sim \frac{k}{M_W} + \frac{M_W}{2k_0}(-1, 0, 0, 1). \tag{61}$$

The first term in ϵ_L gives zero for the coupling of longitudinal W's to massless fermions and so the longitudinal coupling is suppressed by M_W/k_0 relative to the transverse coupling to massless fermions. It is instructive to begin by computing the coupling of a Higgs boson to two longitudinal W bosons, (Fig. 20). The amplitude is given by

$$\mathcal{A}(H \to W_L^+ W_L^-) = g M_W \epsilon_L(p_+) \cdot \epsilon_L(p_-). \tag{62}$$

Using Eq. 60 we have for $M_H >> M_W$,

$$\mathcal{A}(H \to W_L^+ W_L^-) = \frac{g M_H^2}{2 M_W}. \tag{63}$$

The longitudinal coupling of the Higgs boson to W bosons is enhanced for heavy Higgs bosons! It is this fact which makes the process of Fig. 19 relevant.

In order to treat the $W^\pm$ and Z bosons as partons, we consider them as on-shell physical bosons. We make the approximation that the partons have zero transverse

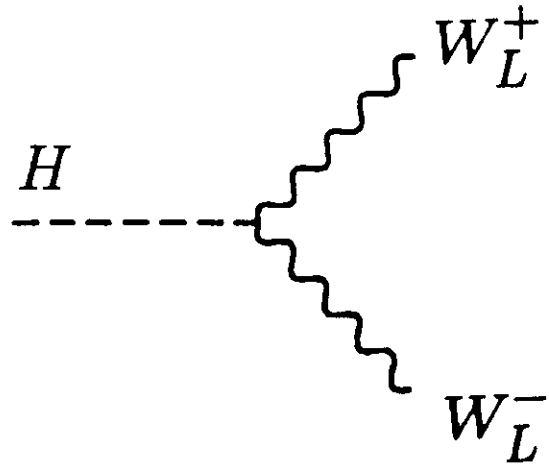

Figure 20: $H \to W_L^+ W_L^-$.

momentum, which ensures that the longitudinal and transverse projections of the W and Z partons are uniquely specified. We want to be able to write a parton level relation ship:

$$\sigma(q_1 + q_2 \to q_1' + X) = \int_{\frac{M_W}{E}}^1 dx f_{q/W}(x)\sigma(W + q_2 \to X). \tag{64}$$

The function $f_{q/W}(x)$ is called the distribution of W's in a quark and it is defined by Eq. 64.

The amplitude for a W with polarization vector ϵ_i to scatter from a quark q_2 to the final state X (see Fig. 21) is:

$$i\mathcal{A}_i(W + q_2 \to X) = \epsilon_i \cdot \mathcal{M}\sqrt{E_q}, \tag{65}$$

where E_q is the quark energy and we have replaced the $W - q_2 - X$ vertex by an effective coupling $\mathcal{M}_\mu\sqrt{E_q}$. Averaging over the quark spin and dropping terms suppressed by M_W^2/E^2, we find

$$d\sigma(W_i + q_2 \to X) = \frac{1}{8k_0} \mid \epsilon_i \cdot \mathcal{M} \mid^2 d\Gamma_X, \tag{66}$$

where the Lorentz invariant phase space of the final state X is $d\Gamma_X$.

We now consider the two body scattering process of Fig. 22 which gives the amplitude,

$$i\mathcal{A}_i(q_1 + q_2 \to q_1' + X) = \frac{g}{2\sqrt{2}}\overline{u}(p')\not{\epsilon}_i^*(1 - \gamma_5)u(p)\epsilon \cdot \mathcal{M}\frac{\sqrt{E_q}}{k^2 - M_W^2}. \tag{67}$$

Because of the factor $1/(k^2 - M_W^2)$, the cross section is dominated by small angles since

$$k^2 \sim E^2(1 - x)\theta^2, \tag{68}$$

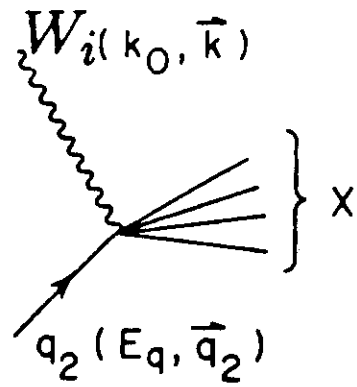

Figure 21: Amplitude for a polarized W to scatter from a quark into the final state X.

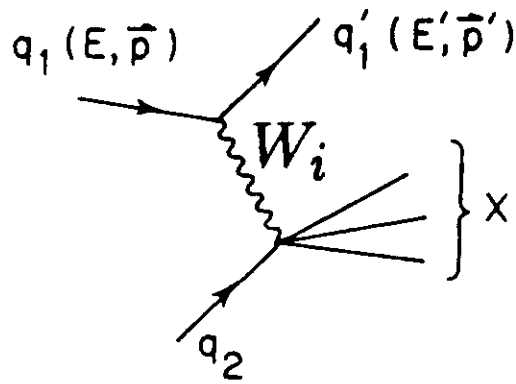

Figure 22: Quark-quark scattering by vector boson exchange.

where θ is the angle between the W and the outgoing quark, q_1'.

The spin averaged total cross section is then

$$\sigma_i(q_1 + q_2 \to q_1' + X) = \frac{1}{32EE_q}\int \frac{d^3p'}{(2\pi)^3}\frac{\mid \mathcal{A}_i(q_1 + q_2 \to q_1' + X)\mid^2}{E'}d\Gamma_X. \qquad (69)$$

The effective W approximation consists of replacing the current, $\mid \epsilon_i \cdot \mathcal{M} \mid$, and the phase space, $d\Gamma_X$, by their values when $k^2 \to M_W^2$ and the W is emitted in the forward direction, $\theta \to 0$. Using the definition of Eq. 64 and the polarizations of Eq. 60 we find the W distributions in a quark from Eq. 69,[31]

$$\begin{aligned} f^L_{q/W}(x) &= \frac{g^2}{8\pi^2}\frac{M_W^2}{E^2}\frac{1}{x}\int \frac{\theta d\theta}{(\theta^2 + \frac{M_W^2}{E^2(1-x)})^2} \\ &= \frac{g^2}{16\pi^2}\frac{1-x}{x} \\ f^T_{q/W}(x) &= \frac{g^2}{64\pi^2 x}\log\left(\frac{4E^2}{M_W^2}\right)\Big[1 + (1-x)^2\Big], \end{aligned} \qquad (70)$$

where we have averaged over the 2 transverse polarizations. The logarithm in Eq. 70 is the same logarithm which appears in the effective photon approximation.[30] The result of Eq. 70 violates our intuition that longitudinal gauge bosons don't couple to massless fermions. However, the integral over $d\theta$ picks out the $\theta \to 0$ region and hence the subleading term in the polarization tensor of Eq. 61.

It is now straightforward to compute the rates for processes involving WW scattering. The hadronic cross section can be written in terms of a luminosity of W's in the proton,

$$\sigma_{pp\to WW\to X}(s) = \int_{\tau_{min}}^1 d\tau \frac{d\mathcal{L}}{d\tau}\mid_{pp/WW}\sigma_{WW\to X}(\tau s) \qquad (71)$$

where the luminosities are defined:

$$\begin{aligned} \frac{d\mathcal{L}}{d\tau}\mid_{pp/WW} &= \sum_{ij}\int_\tau^1 \frac{d\tau'}{\tau'}\int_{\tau'}^1 \frac{dx}{x}f_i(x)f_j\left(\frac{\tau'}{x}\right)\frac{d\mathcal{L}}{d\zeta}\mid_{q_iq_j/WW} \\ \frac{d\mathcal{L}}{d\tau}\mid_{qq/WW} &= \int_\tau^1 \frac{dx}{x}f_{q/W}(x)f_{q/W}\left(\frac{\tau}{x}\right). \end{aligned} \qquad (72)$$

($f_i(x)$ are the quark distribution functions in the proton and $\zeta \equiv \tau/\tau'$). Of course this entire derivation can also be performed for Z bosons. In addition, the luminosities of Eq. 72 can be trivially adapted to find the distribution of gauge bosons in the electron.[33]

In Fig. 23 we show the luminosity of transverse and longitudinal gauge bosons in the proton at the LHC. It is interesting to note that the transverse luminosity is several orders of magnitude larger than the longitudinal luminosity due to the enhancement from the logarithm in $f^T_{q/W}$, as can be seen from Eq. 70 . However, because the coupling of longitudinal gauge bosons to a heavy Higgs boson and to

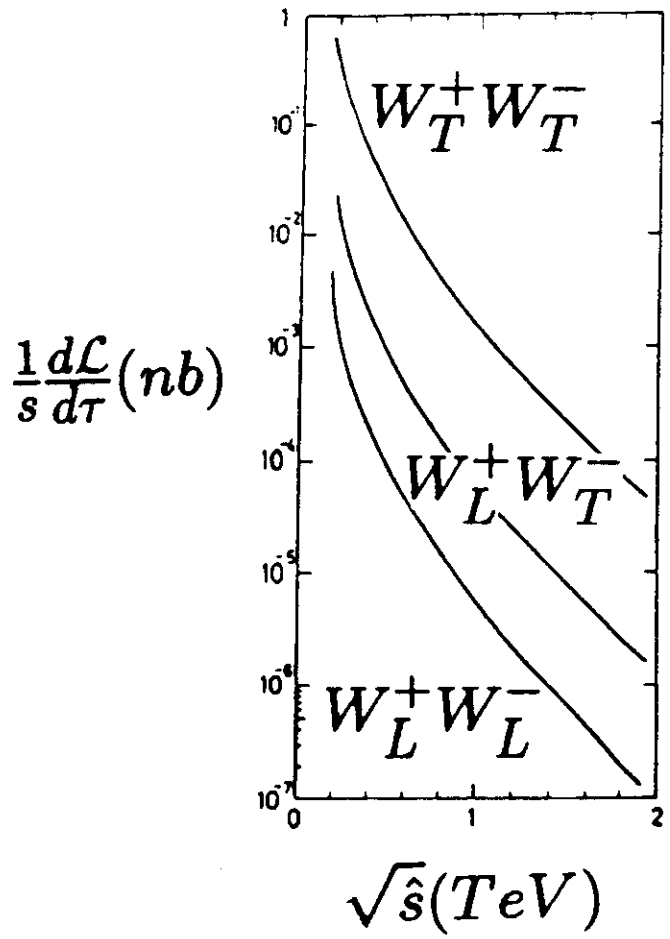

Figure 23: Luminosity of W boson pairs in the proton at the LHC. $\sqrt{\hat{s}}$ is the energy in the W^+W^- center-of-mass. This figure is from Ref. [32].

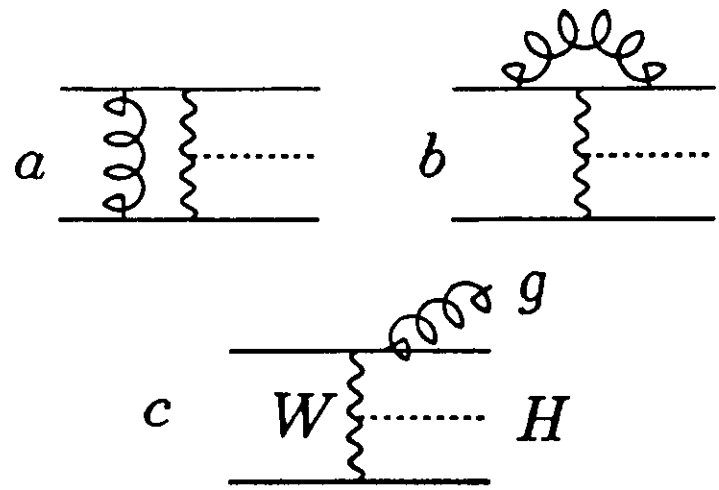

Figure 24: QCD corrections to the effective W approximation.

heavy fermions[9] is enhanced the dominant contribution to a physical process is often from longitudinal gauge boson scattering.

The effective W approximation is particularly useful in models where the electroweak symmetry breaking is due not to the Higgs mechanism, but rather to some strong interaction dynamics (such as technicolor models). In these models one typically estimates the strengths of the 3 and 4 gauge boson couplings due to the new physics. These interactions can then be folded into the luminosity of gauge bosons in the proton (or the electron) to get estimates of the size of the new physics effects.

4.2 Does the Effective W approximation Work?

It is interesting to ask if QCD effects spoil the effective W approximation.[34] Diagrams of the sort shown in Fig. 24 for example cannot be calculated within the context of the effective W approximation. The diagram of Fig. 24a gives a contribution to the cross section of $\mathcal{O}(\alpha_s)$ which is proportional to $Tr(T_A) = 0$. Most of the remaining contributions to the QCD corrections (Figs. 24b and c) can be absorbed in the definition of the structure functions to next to leading order. It has been demonstrated by explicit calculation that the QCD corrections to the effective W approximation are small, of order 10%.[35]

We turn now to a discussion of Higgs boson production from vector boson fusion and compare results obtained with and without the effective W approximation. In the effective W approximation,

$$\sigma(pp \to H) = \frac{16\pi^2}{M_H^3}\Gamma(H \to W^+W^-)\tau\frac{d\mathcal{L}}{d\tau}\,|_{pp/WW}\,. \tag{73}$$

[9]For heavy fermions, the $\overline{\psi}\psi W_L$ coupling is proportional to M_f/M_W.

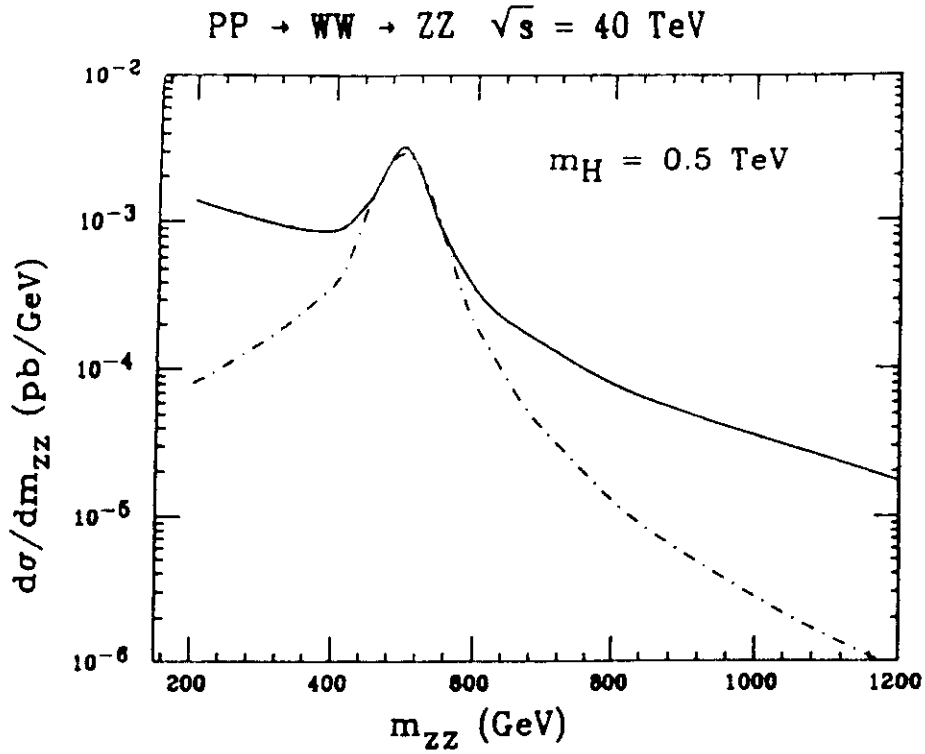

Figure 25: Longitudinal and transverse gauge boson contributions (solid) to $pp \to ZZ$ through intermediate W^+W^- and ZZ interactions for $M_H = 500\ GeV$ at the SSC. The dot-dashed line is the longitudinal contribution alone. This figure is from Ref. [36].

A heavy Higgs boson will quickly decay into W^+W^- pairs with a width

$$\Gamma(H \to W^+W^-) \sim 2\Gamma(H \to ZZ) \sim \frac{G_F M_H^3}{8\sqrt{2}\pi}. \tag{74}$$

As the Higgs mass approaches a TeV, its mass becomes comparable to its width. A useful form to remember is that summed over $W^\pm, Z$,

$$\Gamma(H \to VV) \sim \frac{M_H^3}{2} \quad \text{(TeV units)}. \tag{75}$$

Therefore we cannot consider simply Higgs production for a heavy Higgs boson, but must consider the W^+W^- or ZZ final state where the Higgs boson contributes to an s- channel resonance. All of the diagrams contributing to $VV \to VV$ scattering must be included in order to obtain a gauge invariant result.

There is an extensive literature demonstrating the validity of the effective W approximation at the SSC and we discuss the relevant physics points here.[10] In Fig. 25, we show the contribution of W^+W^- and ZZ scattering to the final state ZZ for both longitudinal and transverse gauge boson intermediate states through the mechanism of Fig. 19 . The Feynman diagrams contributing to the process $W^+W^- \to ZZ$ are shown in Fig. 26. A similar set of diagrams contributes to $ZZ \to ZZ$. It is clear that except for M_{ZZ} near the Higgs pole, it is a poor approximation

[10]Once the validity of the effective W approximation was established for the SSC, theorists didn't bother to redo the calculations for the LHC!

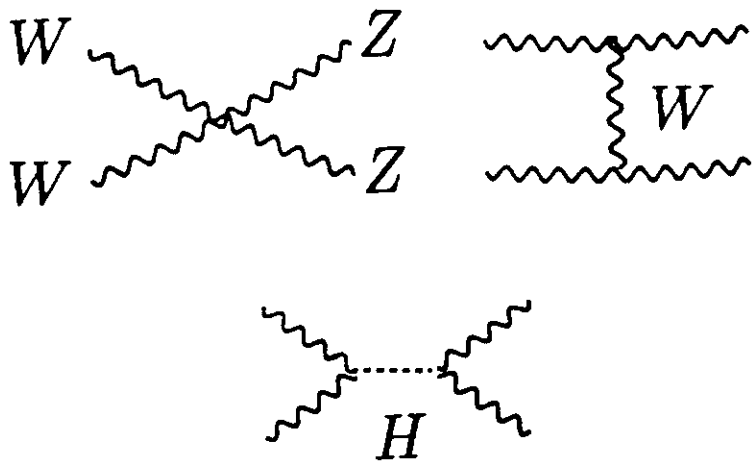

Figure 26: Feynman diagrams contributing to ZZ production from WW fusion.

to keep only the longitudinal modes. Both transverse and longitudinal gauge bosons contribute to the physical amplitude.

We can also investigate whether it makes sense to include only the s-channel Higgs exchange diagram. From Fig. 27 we can see that this is a poor approximation except for M_{WW} near the Higgs boson mass. This figure also includes the contribution to W^+W^- production from the direct scattering $q\bar{q} \to W^+W^-$. This process is often called the background to Higgs production and is much larger than the contribution from W^+W^- scattering. As the Higgs boson becomes increasingly massive, its width becomes wider and the tiny Higgs bump shown in Fig. 27 becomes impossible to observe.

Higgs boson production through vector boson fusion can of course be computed numerically without the use of the effective W approximation. In Fig. 28 we show a comparison of the exact numerical calculation for the process $pp \to WW \to ZZ$ compared with that derived from the effective W approximation. The agreement is excellent and the effective W approximation is accurate to within a factor of two even far from the Higgs pole.[37, 38] This did not have to be the case since the effective W approximation does not contain diagrams where the W is radiated off the incoming or outgoing quark lines (see Fig. 29). We conclude from this series of plots, (Figs. 25, 27 and 28), that the effective W approximation can be used with confidence even away from the Higgs pole if both transverse and longitudinal gauge boson contributions and if all scattering diagrams (not just $s-$ channel Higgs exchange) are included. The most important use of the effective W approximation is the study of very massive, strongly interacting Higgs bosons, which we consider in Section 5.

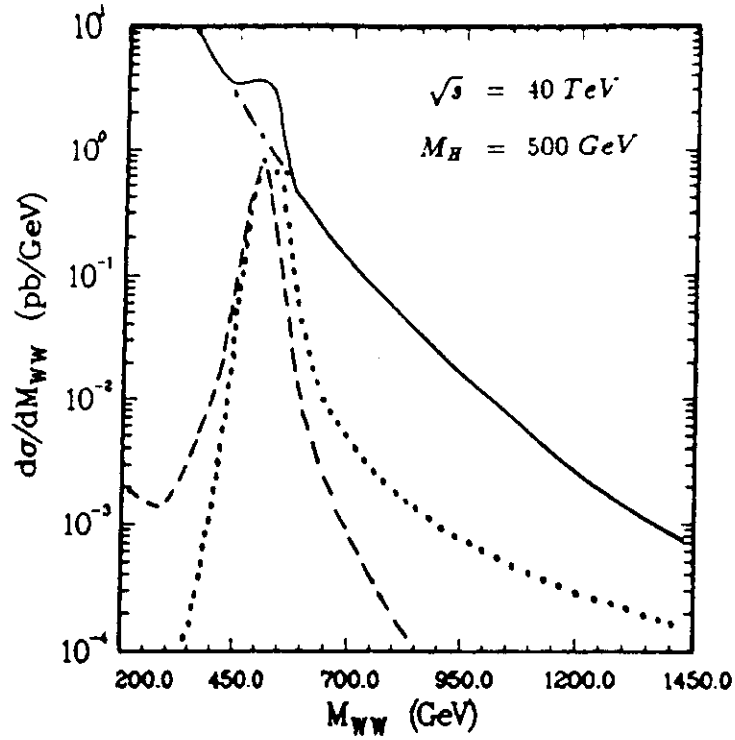

Figure 27: Various contributions to W^+W^- production. The dot- dashed line is the background from $q\bar{q} \to W^+W^-$, the dashed is vector boson scattering and the dotted line is the contribution from s-channel Higgs exchange only. The solid line is the total rate. This figure is from Ref. [36].

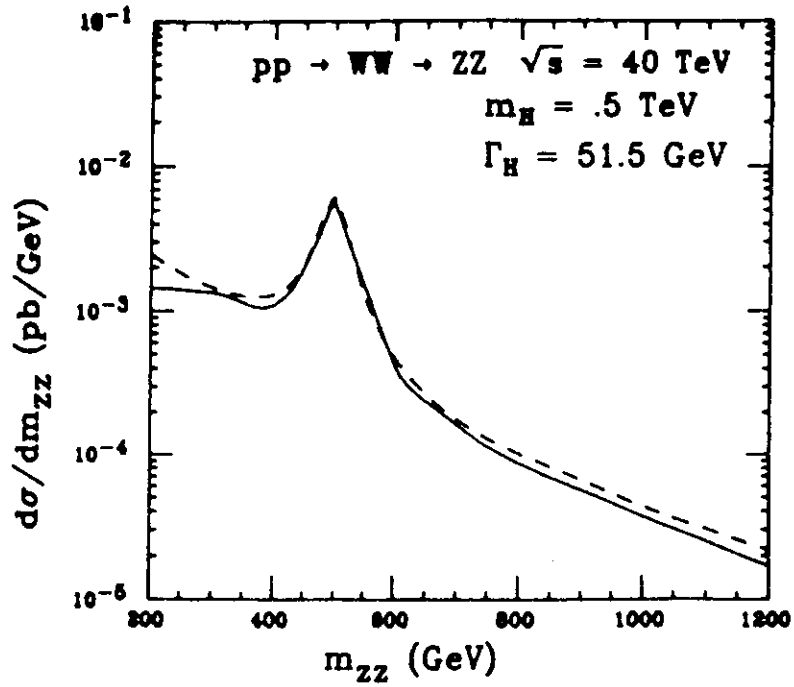

Figure 28: Comparison of the Effective W approximation (dashed) with the exact numerical calculation(solid) for ZZ production from W^+W^- fusion with $|\eta_Z| < 1.5$. This figure is from Ref. [37].

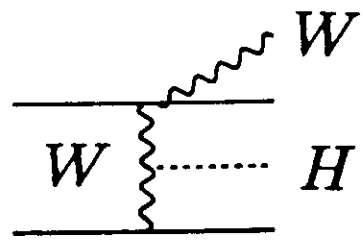

Figure 29: Diagram not contained in the effective W approximation.

4.3 Searching for a Heavy Higgs Boson at the LHC

We now have the tools necessary to discuss the search for a very massive Higgs boson. The various production mechanisms contributing to Higgs production at the LHC are shown in Fig. 30. For $M_H \leqslant 800\ GeV$ the dominant production mechanism at the LHC is gluon fusion, as discussed in Section 3.1. For heavier Higgs masses, the WW fusion mechanism becomes important. Other mechanisms, such as $gg \rightarrow t\bar{t}H$, are quite small at the LHC.[39] It is obvious from Fig. 30 that searching for a Higgs boson on the TeV mass scale will be extremely difficult. For example, a 700 GeV Higgs boson has a cross section near 1 pb leading to around 10^5 events/LHC year. The cleanest way to see these events is the so-called "gold-plated" decay channel,

$$H \rightarrow ZZ \rightarrow l^+l^-l^+l^-. \tag{76}$$

The lepton pairs will reconstruct to the Z mass and the 4 lepton invariant mass will give the Higgs mass. Since the branching ratio, $Z \rightarrow e^+e^- + \mu^+\mu^-$ is $\sim .06$ the number of events for a 700 GeV Higgs is reduced to around 360 four lepton events per year. Since this number will be further reduced by cuts to separate the signal from the background, it is clear that this channel will run out of events as the Higgs mass becomes heavier.[21]

In Fig. 31, we show a Monte Carlo simulation of the capabilities of the ATLAS detector at the LHC to observe a Higgs boson with mass $M_H = 800\ GeV$ through the 4 lepton decay channel.[18] The upper curve shows all of the events including the background from ZZ continuum production. A series of kinematic cuts is applied until the lower curve is reached, where the Higgs bump can be seen. The ATLAS collaboration claims that they will be able to discover the Higgs boson in the mass region $130 < M_H < 800\ GeV$ in the 4 lepton channel. (Similar results are found by the CMS collaboration.[19]).

In order to look for still heavier Higgs bosons, one can look in the decay channel,

$$H \rightarrow ZZ \rightarrow l^+l^-\nu\bar{\nu}. \tag{77}$$

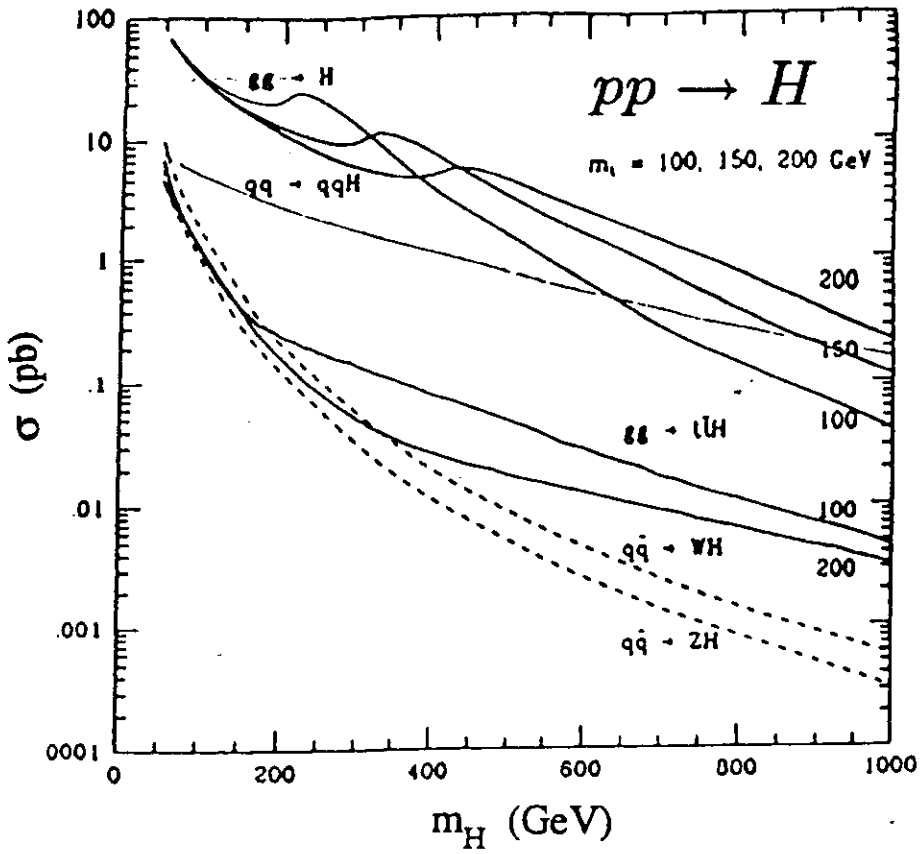

Figure 30: Processes contributing to Higgs production at the LHC.

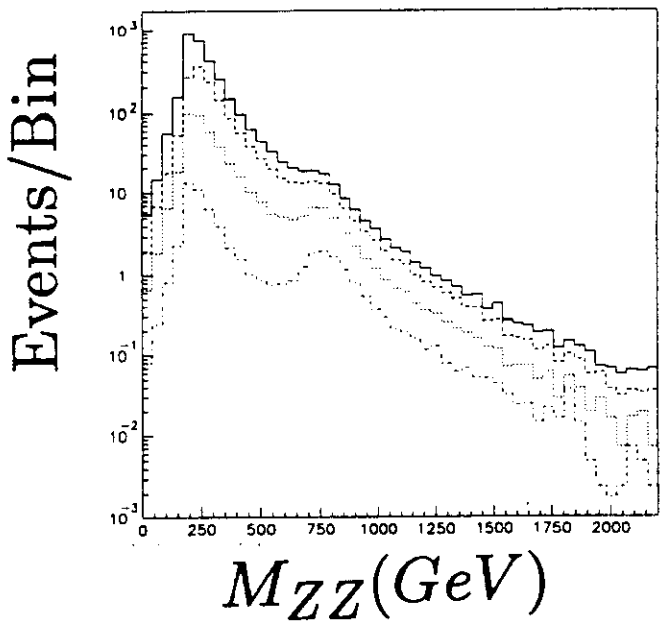

Figure 31: $pp \rightarrow ZZ \rightarrow 4$ leptons for $M_H = 800\ GeV$ at the LHC with the ATLAS detector applying a series of cuts described in the text. This figure is from Ref. [18].

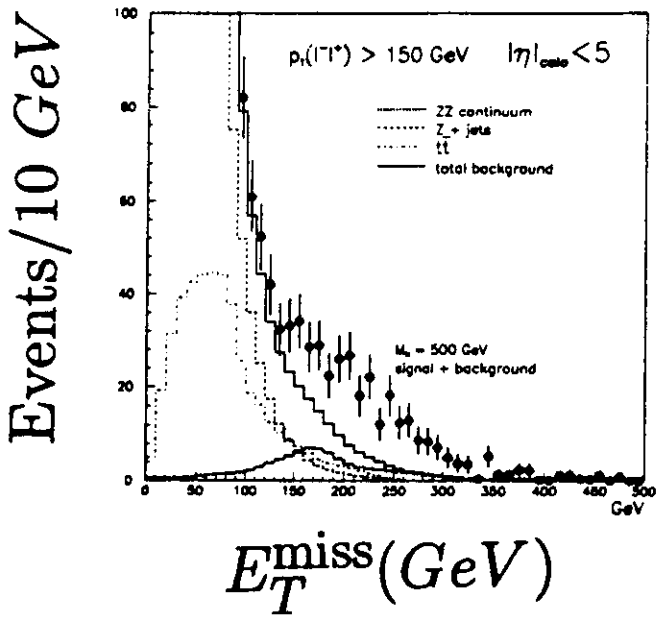

Figure 32: $pp \to ZZ \to l^+l^-\nu\bar{\nu}$ for $M_H = 500\ GeV$ with $\int \mathcal{L} = 10^4 pb^{-1}$ at the LHC using the ATLAS detector. This figure is from Ref. [18].

Since the branching ratio, $Z \to \nu\bar{\nu} \sim 20$ %, this decay channel has a larger rate than the four lepton channel. However, the price is that because of the neutrinos, events of this type cannot be fully reconstructed. An example of this signal is shown in Fig. 32. This channel extends the Higgs mass reach of the LHC slightly.

Another idea which has been proposed is to use the fact that events coming from WW scattering have outgoing jets at small angles, whereas the WW background coming from $q\bar{q} \to W^+W^-$ does not have such jets.[41] Additional sources of background to Higgs detection such as $W+$ jet production have jets at all angles. It is not yet clear whether this idea will be useful in the search for a heavy Higgs.

In this section and in Section 3.3. we have seen that the LHC will have the capability to observe the Higgs boson in the mass region from $100 < M_H < 800\ GeV$. We now return to the Goldstone boson sector of the theory in an attempt to learn something about the Higgs boson in the regime where it is too heavy to be observed at the LHC.

5 Strongly Interacting Higgs Bosons

We can see from the Feynman rules of Fig. 4 that as the Higgs boson becomes heavy, its self interactions become large and it becomes strongly interacting. For $M_H > 1.4\ TeV$, the total Higgs boson decay width is larger than its mass and it no longer makes sense to think of the Higgs boson as a particle. This regime can most easily be studied by going to the Goldstone boson sector of the theory. In Feynman gauge, the three Goldstone bosons, $\omega^{\pm}, z$, have mass $M_{\omega,z} = M_{W,Z}$ and have the

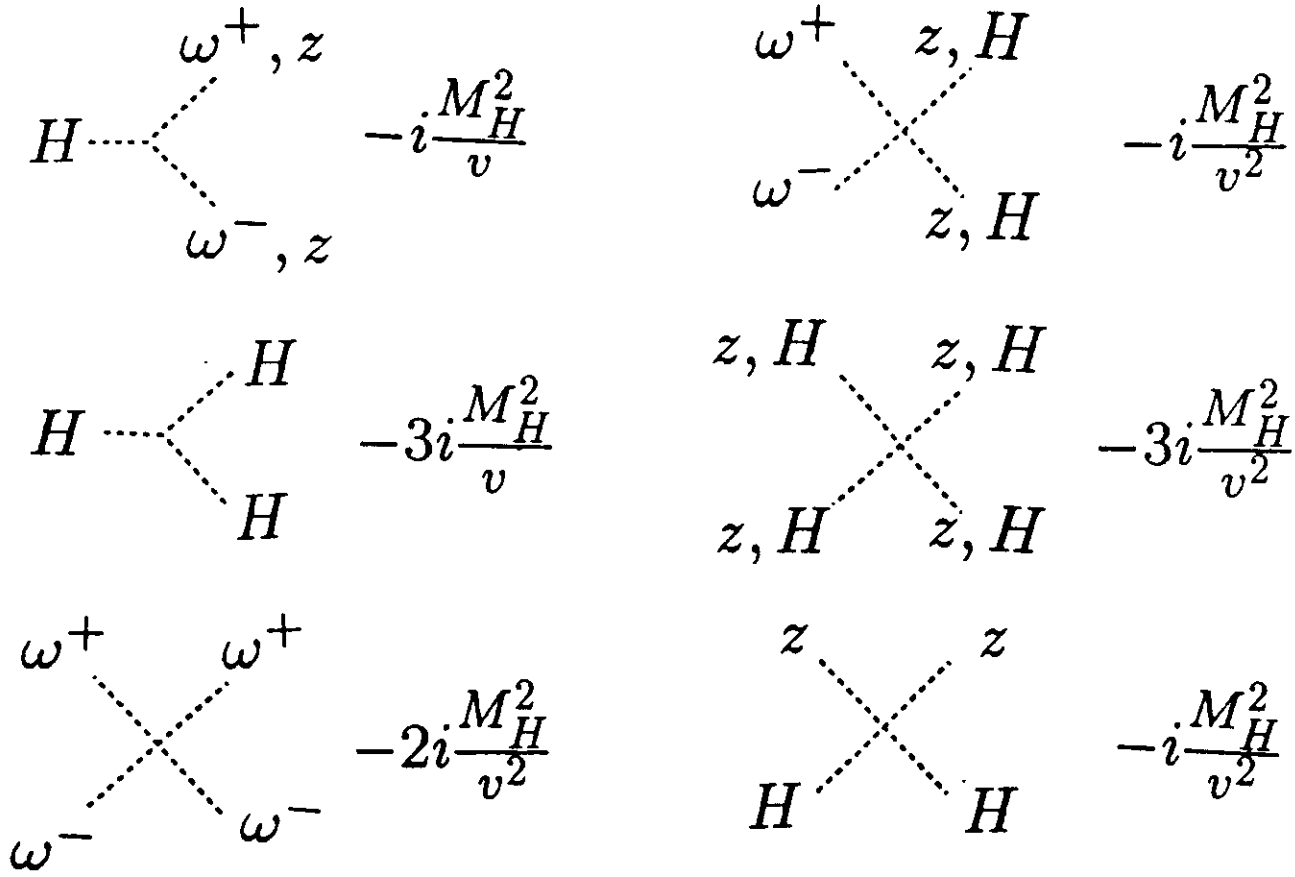

Figure 33: Feynman rules for Higgs-Goldstone boson interactions.

interactions,[42]

$$V = \frac{M_H^2}{2v} H\Big(H^2 + Z^2 + 2\omega^+\omega^-\Big) + \frac{M_H^2}{8v^2}\Big(H^2 + z^2 + 2\omega^+\omega^-\Big)^2. \tag{78}$$

The Feynman rules corresponding to Eq. 78 are given in Fig. 33.

Calculations involving only the Higgs boson and the Goldstone bosons are easy since they involve only scalars. For example the amplitude for $\omega^+\omega^- \to \omega^+\omega^-$[43] can be found from the Feynman diagrams of Fig. 34:

$$\mathcal{A}(\omega^+\omega^- \to \omega^+\omega^-) = -\frac{M_H^2}{v^2}\Big(\frac{s}{s - M_H^2} + \frac{t}{t - M_H^2}\Big), \tag{79}$$

where s, t, u are the Mandelstam variables in the $\omega^+\omega^-$ center of mass frame. It is instructive to compare Eq. 79 with what is obtained by computing $W_L^+W_L^- \to W_L^+W_L^-$ using real longitudinally polarized gauge bosons and extracting the leading power of s from each diagram[44]:

$$\begin{aligned}\mathcal{A}(W_L^+W_L^- \to W_L^+W_L^-) \;=\; & -\frac{1}{v^2}\Big\{-s - t + 2M_Z^2 + \frac{2t}{s}\Big(M_Z^2 - 4M_W^2\Big) + \frac{2M_Z^2 s}{t - M_Z^2} \\ & -8\sin^2\theta_W M_W^2\Big(\frac{M_Z^2 s}{t(t - M_Z^2)}\Big) + \frac{s^2}{s - M_H^2} + \frac{t^2}{t - M_H^2}\Big\}.\end{aligned} \tag{80}$$

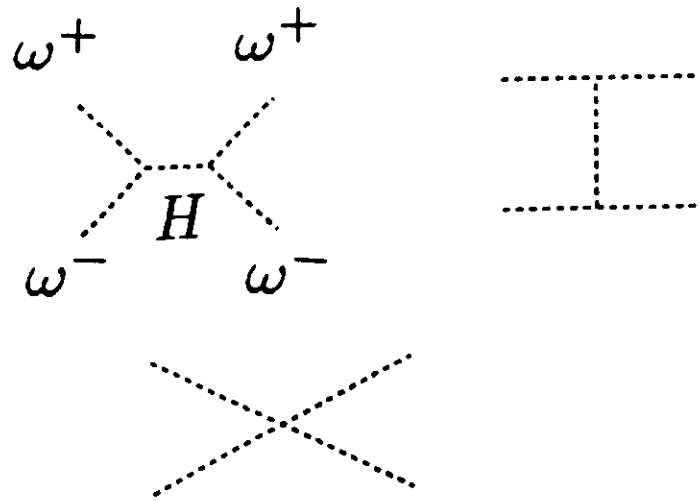

Figure 34: Goldstone boson scattering, $\omega^+\omega^- \to \omega^+\omega^-$.

From Eqs. 79 and 80 we find an amazing result,

$$\mathcal{A}(W_L^+W_L^- \to W_L^+W_L^-) = \mathcal{A}(\omega^+\omega^- \to \omega^+\omega^-) + \mathcal{O}\Big(\frac{M_W^2}{s}\Big). \tag{81}$$

This result means that instead of doing the complicated calculation with real gauge bosons, we can instead do the easy calculation with only scalars if we are at an energy far above the W mass and are interested only in those effects which are enhanced by M_H^2. (The interactions of the transverse gauge bosons are $\mathcal{O}(g^2)$ and have no M_H^2 enhancement.) This is a general result and has been given the name of the electroweak equivalence theorem.[45]

The formal statement of the electroweak equivalence theorem is that

$$\mathcal{A}(V_L^1V_L^2....V_L^N \to V_L^1V_L^2....V_L^{N'}) = (i)^N(-i)^{N'}\mathcal{A}(\omega_1\omega_2...\omega_N \to \omega_1\omega_2...\omega_{N'}) + \mathcal{O}\Big(\frac{M_V^2}{s}\Big), \tag{82}$$

where ω_i is the Goldstone boson corresponding to the longitudinal gauge boson, V_L^i. In other words, when calculating scattering amplitudes of longitudinal gauge bosons at high energy, we can replace the *external* longitudinal gauge bosons by Goldstone bosons. A formal proof of this theorem can be found in Ref. [45].

The electroweak equivalence theorem is extremely useful in a number of applications. For example, to compute the radiative corrections to $H \to W^+W^-$[46] or to $W_L^+W_L^- \to W_L^+W_L^-$[29], the dominant contributions which are enhanced by M_H^2/M_W^2 can be found by computing the one loop corrections to $H \to \omega^+\omega^-$ and to $\omega^+\omega^- \to \omega^+\omega^-$ which involve only scalar particles. Probably the most powerful application of the electroweak equivalence theorem is, however, in the search for the physical effects of strongly interacting gauge bosons which we turn to now.

5.1 $M_H \to \infty$, The Non-Linear Theory

So far we have considered searching for the Higgs boson in various mass regimes. In this section we will consider the consequences of taking the Higgs boson mass much heavier than the energy scale being probed[49]. In fact, we will take the limit $M_H \to \infty$ and assume that the effective Lagrangian for electroweak symmetry breaking is determined by new physics outside the reach of future accelerators such as the LHC. Since we do not know the full theory, we must build the effective Lagrangian out of all operators consistent with the unbroken symmetries. In particular, we must include operators of all dimensions, whether or not they are renormalizable. In this way we construct the most general effective Lagrangian that describes electroweak symmetry breaking.

To specify the effective Lagrangian, we must first fix the pattern of symmetry breaking. We will assume that the global symmetry in the scalar sector of the model is $SU(2)_L \times SU(2)_R$ as in the minimal Standard Model, (see for example, Eq. 78). In this case, the Goldstone bosons can be described in terms of the field[47]

$$\Sigma \equiv e^{\frac{i\omega\cdot\tau}{v}}. \tag{83}$$

This is reminiscent of the Abelian Higgs model where we took,

$$\Phi = \frac{1}{\sqrt{2}} e^{\frac{i\chi}{v}}(H+v). \tag{84}$$

Under the global symmetry the Σ field transforms as,

$$\Sigma \to L^\dagger \Sigma R. \tag{85}$$

It is straightforward to write down the most general $SU(2)_L \times U(1)_Y$ gauge invariant Lagrangian which respects the global symmetry of Eq. 85 and has no more than 2 derivatives acting on the Σ field,

$$\mathcal{L} = \frac{v^2}{4} D_\mu \Sigma^\dagger D^\mu \Sigma - \frac{1}{2} Tr\Big(\hat{W}^{\mu\nu}\hat{W}_{\mu\nu}\Big) - \frac{1}{2} Tr\Big(\hat{B}_{\mu\nu}\hat{B}^{\mu\nu}\Big), \tag{86}$$

where the covariant derivative is given by,

$$D_\mu \Sigma = \partial_\mu \Sigma + \frac{i}{2} g \hat{W}^i_\mu \tau^i \Sigma - \frac{i}{2} g' \hat{B}_\mu \Sigma \tau_3. \tag{87}$$

The gauge field kinetic energies are now matrices:

$$\begin{aligned} \hat{W}_{\mu\nu} &\equiv \frac{1}{2}\Big(\partial_\nu W_\mu - \partial_\mu W_\nu - \frac{i}{2} g [W_\mu, W_\nu]\Big) \\ \hat{B}_{\mu\nu} &= \frac{1}{2}\Big(\partial_\nu B_\mu - \partial_\mu B_\nu\Big)\tau_3 \end{aligned} \tag{88}$$

with $W_\nu \equiv W^i_\nu \cdot \tau_i$. We will also assume a custodial $SU(2)_C$ symmetry.[48] This is the symmetry which forces $\rho = M_W^2/(M_Z^2 \cos\theta_W) = 1$. The pattern of global symmetry

breaking is then $SU(2)_L \times SU(2)_R \to SU(2)_C$. In unitary gauge, $\Sigma = 1$ and it is easy to see that Eq. 86 generates mass terms for the W and Z gauge bosons. The Lagrangian of Eq. 86 is the Standard Model with $M_H \to \infty$.

Using the Lagrangian of Eq. 86 it is straightforward to compute Goldstone boson scattering amplitudes such as[50]

$$\mathcal{A}(\omega^+\omega^- \to zz) = \frac{s}{v^2} \equiv A(s,t,u) \tag{89}$$

which of course agree with those found in the Standard Model when we take $M_H^2 >> s$. Because of the custodial $SU(2)_C$ symmetry, the various scattering amplitudes are related:

$$\begin{aligned}
\mathcal{A}(\omega^+ z \to \omega^+ z) &= A(t,s,u) \\
\mathcal{A}(\omega^+\omega^- \to \omega^+\omega^-) &= A(s,t,u) + A(t,s,u) \\
\mathcal{A}(\omega^+\omega^+ \to \omega^+\omega^+) &= A(t,s,u) + A(u,t,s) \\
\mathcal{A}(zz \to zz) &= A(s,t,u) + A(t,s,u) + A(u,s,t).
\end{aligned} \tag{90}$$

Using the electroweak equivalence theorem, the Goldstone boson scattering amplitudes can be related to the amplitudes for longitudinal gauge boson scattering. The effective W approximation can then be used to find the physical scattering cross sections for hadronic and e^+e^- interactions.

The relationships of Eq. 90 were discovered by Weinberg[50] over 20 years ago for the case of $\pi - \pi$ scattering.[11] Amplitudes which grow with s are a disaster for perturbation theory since eventually they will violate perturbative unitarity as we will discuss in Sec. 6.1. Of course, this simply tells us that there must be some new physics at high energy.

Eq. 86 is a non-renormalizable effective Lagrangian which must be interpreted as an expansion in powers of s/Λ^2, where Λ can be taken to be the scale of new physics (say M_H in a theory with a Higgs boson). At each order in the energy expansion new terms will be generated which will cancel the singularities generated by the order below. To $\mathcal{O}(s^2)$, the infinities which arise at one loop can all be absorbed by defining renormalized parameters, $L_i(\mu)$. The coefficients thus depend on the renormalization scale μ. At $\mathcal{O}(s^2/\Lambda^4)$ we have the interaction terms,

$$\begin{aligned}
\mathcal{L} &= \frac{L_1}{16\pi^2}\Big[Tr\Big(D^\mu\Sigma^\dagger D_\mu\Sigma\Big)\Big]^2 + \frac{L_2}{16\pi^2}\Big[Tr\Big(D^\mu\Sigma^\dagger D_\nu\Sigma\Big)\Big]^2 \\
&\quad -\frac{igL_{9L}}{16\pi^2}Tr\Big(\hat{W}^{\mu\nu}D_\mu\Sigma D_\nu\Sigma^\dagger\Big) - \frac{ig'L_{9R}}{16\pi^2}Tr\Big(\hat{B}^{\mu\nu}D_\mu\Sigma^\dagger D_\nu\Sigma\Big) \\
&\quad +\frac{gg'L_{10}}{16\pi^2}Tr\Big(\Sigma\hat{B}^{\mu\nu}\Sigma^\dagger\hat{W}_{\mu\nu}\Big).
\end{aligned} \tag{91}$$

This is the most general $SU(2)_L \times U(1)_Y$ gauge invariant set of interactions of $\mathcal{O}(1/\Lambda^4)$ which preserves the custodial $SU(2)_C$. The coefficients, L_i have information about the

[11] There is an exact analogy between $\pi\pi$ scattering and $W_L^+W_L^-$ scattering with the replacement $f_\pi \to v$.

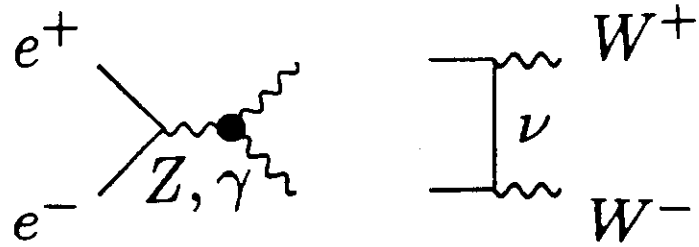

Figure 35: Effects of anomalous gauge boson interactions in e^+e^- interactions.

underlying dynamics of the theory. By measuring the various coefficients one might hope to learn something about the mechanism of electroweak symmetry breaking even if the energy of an experiment is below the scale at which the new physics occurs.

The L_{10} interaction contributes to non-Standard Model 2- and 3-gauge boson interactions. New physics at LEP is often parameterized in terms of the contributions to the gauge boson 2-point functions, (the so-called "oblique corrections"). In a theory without a custodial $SU(2)_C$ symmetry, there are three possible interactions, often called S,T, and U.[55] Since we have assumed a custodial $SU(2)_C$ symmetry, there is only one interaction contributing to non-Standard Model 2- gauge boson interactions and we have

$$L_{10}(M_Z) = -\pi S. \tag{92}$$

The L_{10} interaction contributes to $\gamma - Z$ mixing and is limited by precision electroweak measurements at LEP:[54, 57]

$$-1.1 < L_{10}(M_Z) < 1.8 \tag{93}$$

at the 90 % confidence level from measurements of the total Z width. The L_{9L}, L_{9R} and L_{10} coefficients all contribute to 3 gauge boson interactions, while the L_1, L_2, L_{9L}, and L_{9R} interactions contribute to 4 gauge boson interactions. Within this framework the 2,3, and 4-point gauge boson interactions are related by the gauge invariance of Eq. 91.

Effects of the new interactions can be looked for in e^+e^- interactions, as in Fig. 35. At high energy, there is a delicate cancellation between t- channel ν exchange and s- channel γ and Z exchange in the process $e^+e^- \rightarrow W^+W^-$.[51] If this cancellation is spoiled there is a contribution to the cross section which grows with energy.[53] The Lagrangian of Eq. 91 contributes terms which grow with s to the 3 gauge boson vertices shown in Fig. 35 which is potentially measurable at LEPII. Unfortunately, these effects tend to be rather small in all models which have been considered.

The effects of the non-standard model couplings of Eq. 91 can also be searched for in hadron machines which are sensitive to both the three and four gauge boson

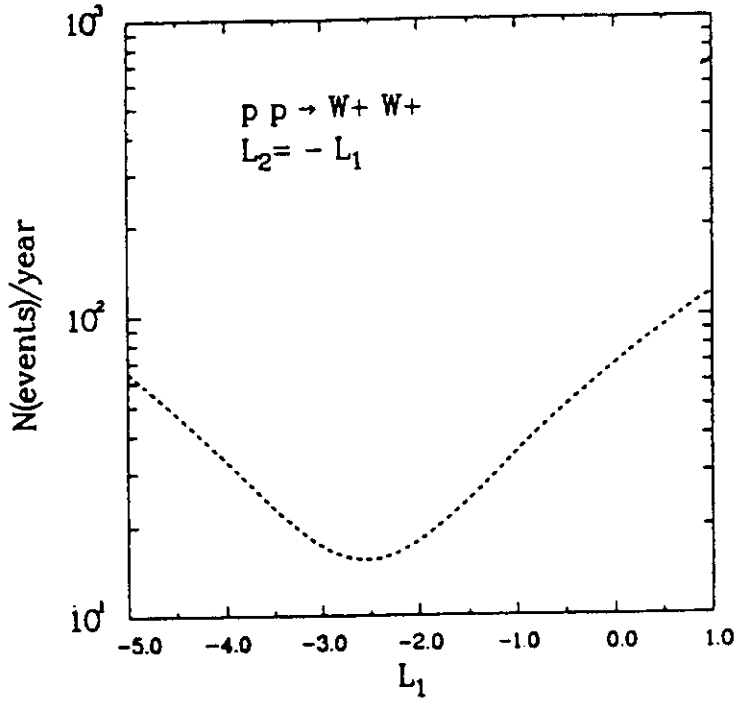

Figure 36: Strong interaction effects in hadronic collisions. The dotted line is the number of $W_L^+W_L^+$ events at the LHC from vector boson fusion with $\int \mathcal{L} = 10^{40}/cm^2$ for $.5 < M_{WW} < 1\ TeV$. We have assumed $L_2 = -L_1$ with all other $L_i = 0$ and a renormalization scale $\mu = 1.5\ TeV$.

vertices.[56, 59, 60, 61] To study strong interactions with the Lagrangian of Eq. 91 one must use the effective W approximation to get results for pp scattering. This has the result that the calculation has a rather limited region of validity,

$$M_W^2 < \hat{s} < \Lambda^2. \tag{94}$$

In Fig. 36, we show the effects at the LHC of turning on small values of the L_i as compared to the lowest order result and see that the effects are quite small.[12] We define a signal as "observable" if it induces a change in the integrated cross section of greater than 50%, which implies that the LHC will be sensitive to $| L_i | > 1$. (More precise values can be found in Ref. [59, 60].)

5.2 Coefficients of New Interactions in a Strongly Interacting Symmetry Breaking Sector

It is instructive to estimate the size of the L_i coefficients in typical theories. Using the effective Lagrangian approach this can be done in a consistent way. We first consider a model in which we couple the Goldstone bosons to a scalar, isoscalar resonance like the Higgs boson. We assume that the L_i are dominated by tree-level exchange of the scalar boson. By integrating out the scalar particle and matching coefficients at the

[12]The W^+W^+ channel is advantageous in the search for strongly interacting symmetry breaking effects since there is no $q\bar{q}$ background.

scale M_H, we find[58]

$$\begin{aligned} L_1(\mu) &= \frac{64\pi^3\Gamma_H v^4}{3}\frac{1}{M_H^5} + \frac{1}{24}\log\Big(\frac{M_H^2}{\mu^2}\Big) \\ L_2(\mu) &= L_{9L}(\mu) = L_{9R}(\mu) = -L_{10}(\mu) = \frac{1}{12}\log\Big(\frac{M_H^2}{\mu^2}\Big), \end{aligned} \tag{95}$$

where Γ_H is the width of the scalar into Goldstone bosons. If we naively take

$$\Gamma_H = \frac{3M_H^3}{32\pi v^2} \tag{96}$$

as in the Standard Model, we find for $M_H = 2\ TeV$ and $\mu = 1.5\ TeV$, $L_1 = .33$ and $L_2 = .01$.

We can also consider a second model for the L_i and assume that the coefficients are dominated by tree-level exchange of a ρ-like particle with spin and isospin one. Integrating out the ρ and matching coefficients at the scale M_ρ we find[58]

$$\begin{aligned} L_1(\mu) &= \frac{1}{24}\Big[-\frac{96\pi^2 f^2}{M_\rho^2} + \log\Big(\frac{M_\rho^2}{\mu^2}\Big)\Big] \\ L_2(\mu) &= \frac{1}{12}\Big[\frac{48\pi^2 f^2}{M_\rho^2} + \log\Big(\frac{M_\rho^2}{\mu^2}\Big)\Big] \\ L_{9L}(\mu) = L_{9R}(\mu) &= \frac{1}{12}\Big[\frac{96\pi^2 f F_\rho}{M_\rho^2} + \log\Big(\frac{M_\rho^2}{\mu^2}\Big)\Big] \\ L_{10}(\mu) &= -\frac{1}{12}\Big[\frac{48\pi^2 F_\rho^2}{M_\rho^2} + \log\Big(\frac{M_\rho^2}{\mu^2}\Big)\Big] \end{aligned} \tag{97}$$

where the constant f is related to the width Γ_ρ,

$$\Gamma_\rho = \frac{1}{48\pi}\frac{f^2}{v^4}M_\rho^3 \tag{98}$$

and F_ρ is defined by

$$\langle 0 \mid V_\mu^i \mid \rho^k(p)\rangle = \delta^{ik}\epsilon_\mu F_\rho M_\rho. \tag{99}$$

We can use large N scaling arguments to estimate f and F_ρ. For $M_\rho = 2\ TeV$ and $\mu = 1.5\ TeV$, we find $L_1 = -.31$, $L_2 = .38$, $L_9 = 1.4$ and $L_{10} = -1.5$. Since we estimated that the LHC will be sensitive to $\mid L_i \mid < 1$, we see that the LHC will indeed probe electroweak symmetry breaking in the TeV region.

One can estimate the amount of time it would take to see a signal of a strongly interacting electroweak symmetry breaking sector at the LHC. The signal has no resonance shape and will be a small excess of events over that predicted from the lowest order Lagrangian of Eq. 86. For example, a model with the L_i having values corresponding to a 2.5 TeV techni-rho would only be observable at the LHC with five years of running! (and then there would be only 14 signal events in the optimal W^+Z channel!).[61] It is clear that this is an extremely difficult way in which to look for evidence of the Higgs boson.

6 Indirect Limits on the Higgs Boson Mass

In the first sections of this report we have systematically discussed how to search experimentally for the Higgs boson in the various mass regimes. We now take a different tack and ask what we can learn about the Higgs boson through indirect measurements

6.1 Unitarity

In the previous section we discussed looking for strongly interacting Higgs bosons through effects which grow with the energy. However, models which have cross sections rising with s will eventually violate perturbative unitarity. To see this we consider $2 \rightarrow 2$ elastic scattering. The differential cross section is

$$\frac{d\sigma}{d\Omega} = \frac{1}{64\pi^2 s} \mid \mathcal{A} \mid^2 . \tag{100}$$

Using a partial wave decomposition the amplitude can be written as

$$\mathcal{A} = 16\pi \sum_{l=0}^{\infty} (2l+1) P_l(\cos\theta) a_l \tag{101}$$

where a_l is the spin l partial wave and P_l are the Legendre polynomials. The cross section can now be written as

$$\begin{aligned} \sigma &= \frac{8\pi}{s} \sum_{l=0}^{\infty} \sum_{l'=0}^{\infty} (2l+1)(2l'+1) a_l a_l^* \\ &\quad \cdot \int_{-1}^{1} d\cos\theta P_l(\cos\theta) P_{l'}(\cos\theta) \\ &= \frac{16\pi}{s} \sum_{l=0}^{\infty} (2l+1) \mid a_l \mid^2 \end{aligned} \tag{102}$$

where we have used the fact that the P_l's are orthogonal. The optical theorem gives,

$$\sigma = \frac{1}{s} Im\Big[\mathcal{A}(\theta = 0)\Big] = \frac{16\pi}{s} \sum_{l=0}^{\infty} (2l+1) \mid a_l \mid^2 . \tag{103}$$

This immediately yields the unitarity requirement which is illustrated in Fig. 37.

$$\mid a_l \mid^2 = Im(a_l). \tag{104}$$

From Fig. 37 we see that one statement of unitarity is the requirement that

$$\mid Re(a_l) \mid < \frac{1}{2}. \tag{105}$$

As a demonstration of unitarity restrictions we consider the scattering of longitudinal gauge bosons, $W_L^+ W_L^- \rightarrow W_L^+ W_L^-$, which can be found to $\mathcal{O}(M_W^2/s)$ from the

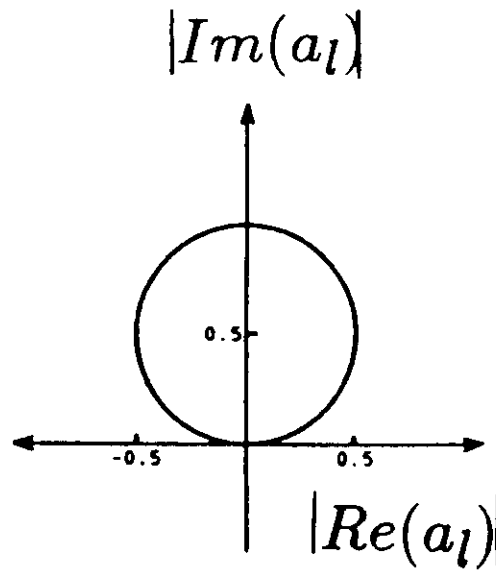

Figure 37: Argand diagram showing unitarity condition on scattering amplitudes.

Goldstone boson scattering of Fig. 34. We begin by constructing the $J = 0$ partial wave in the limit $M_W^2 << s$ from Eq. 79,

$$\begin{aligned} a_0^0(\omega^+\omega^- \to \omega^+\omega^-) &\equiv \frac{1}{16\pi s}\int_{-s}^{0} \mid \mathcal{A} \mid dt \\ &= -\frac{G_F M_H^2}{8\sqrt{2}\pi}\left[2 + \frac{M_H^2}{s - M_H^2} - \frac{M_H^2}{s}\log\left(1 + \frac{s}{M_H^2}\right)\right]. \end{aligned} \quad (106)$$

If we go to very high energy, $s >> M_H^2$, then Eq. 106 has the limit

$$a_0^0(\omega^+\omega^- \to \omega^+\omega^-) \longrightarrow_{s>>M_H^2} -\frac{G_F M_H^2}{4\pi\sqrt{2}}. \quad (107)$$

Applying the unitarity condition, $\mid Re(a_0^0) \mid < \frac{1}{2}$ gives the restriction

$$M_H < 860\ GeV. \quad (108)$$

It is important to understand that this does not mean that the Higgs boson cannot be heavier that 860 GeV, it simply means that for heavier masses perturbation theory is not valid. By considering coupled channels, a slightly tighter bound than Eq. 108 can be obtained. The Higgs boson therefore plays a fundamental role in the theory since it cuts off the growth of the partial wave amplitudes and makes the theory unitary.

We can apply the alternate limit to Eq. 106 and take the Higgs boson much heavier than the energy scale. In this limit[62]

$$a_0^0(\omega^+\omega^- \to \omega^+\omega^-) \longrightarrow_{s<<M_H^2} \frac{G_F s}{16\pi\sqrt{2}}. \quad (109)$$

Again applying the unitarity condition we find,

$$\sqrt{s_c} < 1.8\ TeV \tag{110}$$

We have used the notation s_c to denote s(critical), the scale at which perturbative unitarity is violated. Eq. 110 is the basis for the oft-repeated statement," *There must be new physics on the TeV scale*". Eq. 110 is telling us that without a Higgs boson, there must be new physics which restores perturbative unitarity somewhere below an energy scale of 1.8 TeV.

6.2 Triviality

Bounds on the Higgs boson mass have also been deduced on the grounds of *triviality*.[63] The basic argument goes as follows: Consider a pure scalar theory in which the potential is given by[13]

$$V(\Phi) = \mu^2\Phi^\dagger\Phi + \lambda(\Phi^\dagger\Phi)^2 \tag{111}$$

where the quartic coupling is

$$\lambda = \frac{M_H^2}{2v^2}. \tag{112}$$

This is the scalar sector of the Standard Model with no gauge bosons or fermions. The quartic coupling runs with renormalization scale Q:

$$\frac{d\lambda}{dt} = \frac{3\lambda^2}{4\pi^2}, \tag{113}$$

where $t \equiv \log(Q^2/Q_0^2)$ and Q_0 is some reference scale. (The reference scale is often taken to be v in the Standard Model.) Eq. 113 is easily solvable,

$$\begin{aligned} \frac{1}{\lambda(Q)} &= \frac{1}{\lambda(Q_0)} - \frac{3}{4\pi^2}\log\left(\frac{Q^2}{Q_0^2}\right), \\ \lambda(Q) &= \frac{\lambda(Q_0)}{\left[1 - \frac{3\lambda(Q_0)}{4\pi^2}\log(\frac{Q^2}{Q_0^2})\right]}. \end{aligned} \tag{114}$$

From Eq. 114 we see that $\lambda(Q)$ blows up as $Q \to \infty$ (called the Landau pole). Regardless of how small $\lambda(Q_0)$ is, $\lambda(Q)$ will eventually become infinite at some large Q. Alternatively, $\lambda(Q_0) \to 0$ as $Q \to 0$ with $\lambda(Q) > 0$. Without the $\lambda\Phi^4$ interaction of Eq.111 the theory becomes a non-interacting theory at low energy, termed a trivial theory. Of course, this picture is valid only if the one loop evolution equation of Eq. 113 is an accurate description of the theory at large λ. For large λ, however, higher order or non-perturbative corrections to the evolution equation must be included to determine if triviality really is a problem for the Standard Model.

There are many variations on the triviality theme which attempt to place bounds on the Higgs mass and we will describe several of them here. Suppose we consider

[13] $\mu^2 < 0,\ \lambda > 0$.

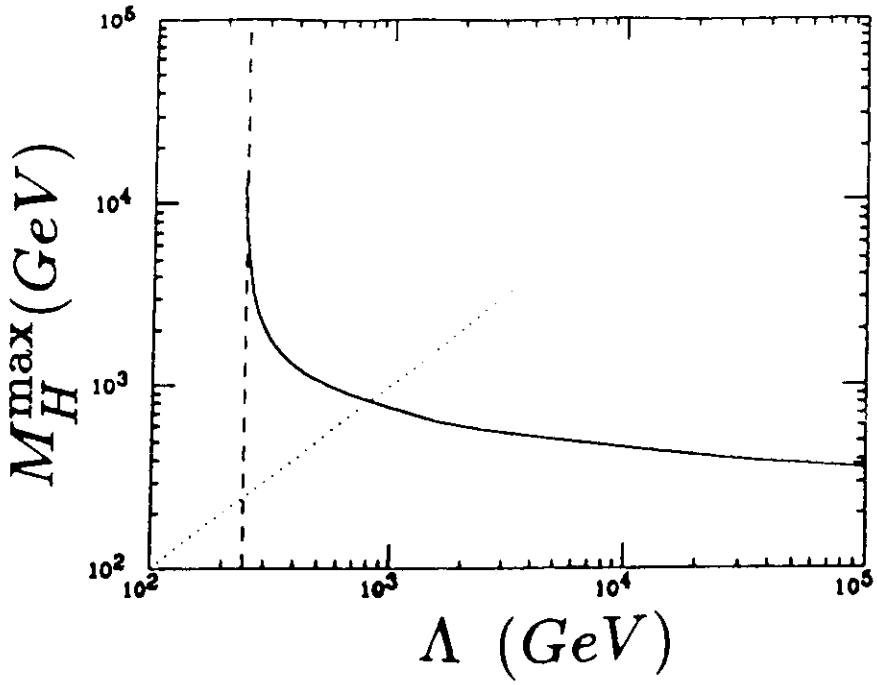

Figure 38: Upper bound on the Higgs mass in a pure Φ^4 theory. The solid line is the result of Eq. 115. The dashed line is $\Lambda = v$ and the dotted line $\Lambda = M_H^{\max}$.

a theory with only scalars and assume that there is some new physics at a scale $\Lambda < M_{Pl}$. Then if we take $\lambda(\Lambda)$ to have its maximum value (∞) and evolve the coupling down to the weak scale (v) we will find the maximum allowed value of the Higgs mass,

$$\lambda(v) = \frac{M_H^2(\max)}{2v^2} = \frac{4\pi^2}{3\log(\frac{\Lambda^2}{v^2})}. \tag{115}$$

Scenarios like this tend to get bounds on the order of $M_H < \mathcal{O}(400 - 1000\ GeV)$ as illustrated in Fig. 38. Since this picture clearly only makes sense for $M_H < \Lambda$, we have also shown the $\Lambda = M_H^{\max}$ curve in Fig. 38 and we see that for $\Lambda < 1\ TeV$, this procedure for limiting the Higgs boson mass breaks down. However, this breakdown leads to the exciting possibility of new physics in the TeV region which should be experimentally accessible at the LHC. Note that as $\Lambda \to \infty$, $M_H^{\max}$ quickly reaches its asymptotic value since the sensitivity of the limit to the cutoff is only logarithmic. If we apply an arbitrary cutoff of $(\Lambda_{cut}/M_H) > 2\pi$, we find a limit $M_H < 930\ GeV$ from Eq. 115.

Lattice gauge theory calculations have used similar techniques to obtain a bound on the Higgs mass.[64] One criticism of the previous bounds could be that it makes no sense to use one loop perturbation theory in the limit $\lambda \to \infty$. Non-perturbative lattice gauge theory calculations overcome this deficit. As above, they consider a purely scalar theory and require that the scalar self coupling λ remain finite for all scales less than $2\pi M_H$. This gives a limit[65]

$$M_H(\text{lattice}) < 640\ GeV. \tag{116}$$

The lattice results are relatively insensitive to the value of the cutoff chosen, as can

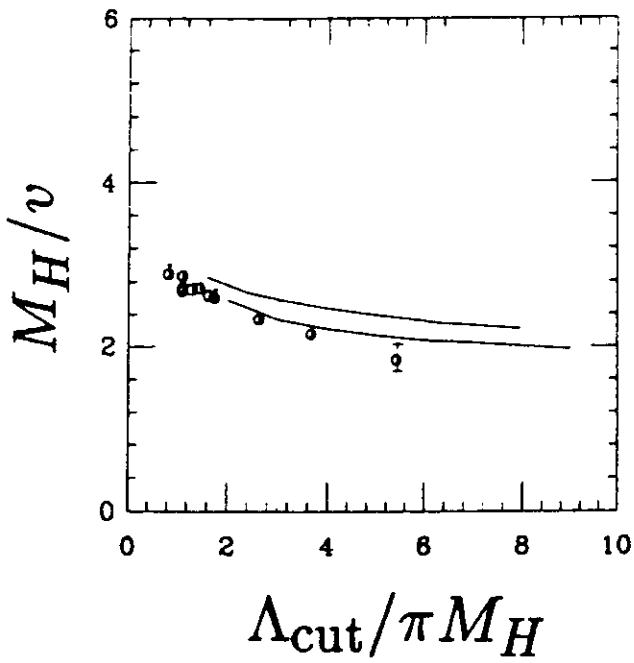

Figure 39: Lattice gauge theory bound on the Higgs boson mass. This figure is from Ref. [65].

be seen in Fig. 39. It is interesting that all of the limits based on the running of the pure scalar theory tend to be in the 1 TeV range, as was the unitarity bound.

Of course everything we have done so far is for a theory with only scalars. The physics changes dramatically when we couple the theory to fermions and gauge bosons. Since the Higgs coupling to fermions is proportional to the Higgs boson mass, the only relevant fermion is the top quark. When we include the top quark and the gauge bosons, Eq. 113 becomes[66]

$$\beta_\lambda \equiv \frac{d\lambda}{dt} = \frac{1}{16\pi^2}\left[12\lambda^2 + 6\lambda h_t^2 - 3h_t^4 - \frac{3}{2}\lambda(3g^2 + g'^2) + \frac{3}{16}(2g^4 + (g^2 + g'^2)^2)\right] \quad (117)$$

where $h_t \equiv \sqrt{2}M_T/v$. The important physics point is the opposite signs between the various terms. For a heavy Higgs boson , $\lambda > h_t, g, g'$, and

$$\frac{d\lambda}{dt} \sim \frac{\lambda}{16\pi^2}\left[12\lambda + 6h_t^2 - \frac{3}{2}(3g^2 + g'^2)\right]. \quad (118)$$

There is a critical value of λ which depends on the top quark mass,

$$\lambda_c \equiv \frac{1}{8}(3g^2 + g'^2) - \frac{h_t^2}{2} \quad (119)$$

for which there is no evolution of the scalar coupling constant.[67] If $M_H > M_H^c \equiv \sqrt{2\lambda_c}v$ then the quartic coupling blows up and the theory is non-perturbative. If we require that the theory be perturbative (i.e., the Higgs quartic coupling be finite) at all energy scales below some unification scale ($\sim 10^{16}$ GeV) then an upper bound on the Higgs mass is obtained as a function of the top quark mass. For $M_T = 170$ GeV

this bound is $M_H < 170\ GeV$. [67] If a Higgs boson were found which was heavier than this bound, it would require that there be some new physics below the unification scale. We see that the inclusion of the top quark into the evolution equations for the scalar coupling has changed the bounds on the Higgs mass considerably. Of course this analysis relies on the use of the one-loop evolution equations. As yet, there is no lattice bound on the Higgs mass which incorporates a heavy top quark mass.

6.3 Vacuum Stability

A bound on the Higgs mass can also be derived by the requirement that spontaneous symmetry breaking actually occurs;[68] that is,

$$V(v) < V(0). \tag{120}$$

For small λ, Eq. 117 can be solved to find

$$\lambda(Q) = \lambda(Q_0) + \beta_\lambda \log\Big(\frac{Q^2}{Q_0^2}\Big), \tag{121}$$

where the small λ limit of β_λ can be found from Eq. 117. If we substitute this into the potential, we find

$$V(\Phi) \sim \mu^2 \Phi^\dagger \Phi + \lambda(Q_0)(\Phi^\dagger \Phi)^2 + \beta_\lambda (\Phi^\dagger \Phi)^2 \log\Big(\frac{Q^2}{Q_0^2}\Big). \tag{122}$$

We can find the minimum of the potential by taking

$$\frac{\partial V}{\partial \Phi} \mid_{\Phi = v/\sqrt{2}} = 0. \tag{123}$$

Taking the second derivative of the potential and substituting in the requirement of Eq. 123 we find the Higgs mass

$$M_H^2 = \frac{1}{2}\frac{\partial^2 V}{\partial \Phi^2} \mid_{\phi = v/\sqrt{2}}. \tag{124}$$

The requirement of Eq. 120 that spontaneous symmetry breaking occurs gives the famous Coleman-Weinberg bound,[68]

$$M_H^2 > \beta_\lambda v^2 = \frac{3}{16\pi^2 v^2}\Big(2M_W^4 + M_Z^4 - 4M_T^4\Big). \tag{125}$$

For $M_T > 78\ GeV$, $\beta_\lambda < 0$ and the potential turns over and is unbounded below. Of course perturbation theory breaks down for $\Phi \to \infty$ and the one loop results are not valid.

A more careful analysis [69] using the 2 loop renormalization group improved effective potential[14] and the running of all couplings gives the requirement from vacuum

[14]The renormalization group improved effective potential sums all potentially large logarithms, $\log(Q^2/Q_0^2)$.

stability,[70][15]

$$M_H(GeV) > 132 + 2.2(M_T - 170) - 4.5\Big(\frac{\alpha_s - .117}{.007}\Big). \tag{126}$$

We see that when λ is small (a light Higgs boson) radiative corrections become important and lead to a lower limit on the Higgs boson mass from the requirement of vacuum stability. If λ is large (a heavy Higgs boson) then unitarity and triviality arguments lead to an upper bound on the Higgs mass.

6.4 Bounds from Electroweak Radiative Corrections

The Higgs boson enters into one loop radiative corrections in the standard model and we might hope that precision electroweak measurements would give some bound on the Higgs mass. For example the ρ parameter gets a contribution from the Higgs boson[71][16]

$$\rho = 1 - \frac{11g^2}{96\pi^2}\tan^2\theta_W \log\Big(\frac{M_H}{M_W}\Big). \tag{127}$$

In fact it is straightforward to demonstrate that at one loop all electroweak parameters have at most a logarithmic dependance on M_H.[49] This fact has been glorified by the name of the "screening theorem".[72] In general, electroweak radiative corrections involving the Higgs boson take the form,

$$g^2\Big(\log\frac{M_H}{M_W} + g^2\frac{M_H^2}{M_W^2}\ldots\Big). \tag{128}$$

That is, effects quadratic in the Higgs mass are always screened by an additional power of g relative to the lower order logarithmic effects and so radiative corrections involving the Higgs boson can never be large.[73] We can demonstrate this in terms of the non-linear model discussed in Section 5.1 where the Higgs boson was removed from the theory. One loop corrections to this theory give divergences which can correctly be interpreted as the $\log(M_H)$ terms of the Standard Model loops.

From precision measurements at LEP of electroweak observables there is only the very weak bound on the Higgs boson mass,[74]

$$M_H < 780\ GeV \quad (90\%\ \text{confidence level}), \tag{129}$$

although χ^2 fits to the data tend to prefer light Higgs masses. From the LEP data alone, the minimum of the χ^2 fit to the top quark mass and the Higgs mass is at $M_H = 60$ GeV, while if the CDF measurement of the top quark mass is included the χ^2 minimum occurs at $M_H = 120\ GeV$.

[15]This limit requires that the vacuum be stable up to very large scales, $\sim 10^{15}\ GeV$.

[16]This result is scheme dependent. Here $\rho \equiv M_W^2/M_Z^2\cos^2\theta_W(M_W)$, where $\cos\theta_W$ is a running parameter calculated at an energy scale of M_W.

7 Problems with the Higgs Mechanism

In the preceeding sections we have discussed many features of the Higgs mechanism. However, many theorists firmly believe that the Higgs mechanism cannot be the entire story behind electroweak symmetry breaking. The primary reasons are:

- The Higgs sector of the theory is trivial.
- The Higgs mechanism doesn't explain why $v = 246\ GeV$.
- The Higgs mechanism doesn't explain why fermions have the masses they do.
- Loop corrections involving the Higgs boson are quadratically divergent and counterterms must be adjusted order by order in perturbation theory to cancel these divergences. This fine tuning is considered by most theorists to be unnatural.

In light of the many objections to the simplest version of the Higgs mechanism theorists have considered several alternatives to the Higgs mechanism for electroweak symmetry breaking. One proposal, that the electroweak symmetry be broken dynamically by a mechanism such as technicolor has been discussed at this school by Appelquist.[75] Another alternative to the standard model Higgs mechanism is that the Standard Model becomes supersymmetric. The electroweak symmetry is still broken by the Higgs mechanism, but the quadratic divergences in the scalar sector are cancelled automatically because of the expanded spectrum of the theory and so the model is no longer considered to be unnatural. In the next section, we will briefly discuss the phenomenology of the Higgs bosons occurring in supersymmetric models and emphasize the similarity of much of the phenomenology to that of the Standard Model Higgs. The theoretical underpinning of supersymmetric models has been presented at this school by Ramond.[76]

8 Higgs Bosons in Supersymmetric Models

In the standard (non-supersymmetric) model of electroweak interactions, the fermion masses are generated by Yukawa terms in the Lagrangian

$$\mathcal{L} = -\lambda_d \overline{Q}_L \Phi d_R - \lambda_u \overline{Q}_L \Phi^c u_R + h.c. \tag{130}$$

In a supersymmetric theory however, a term proportional to Φ^c is not allowed[17] and so another scalar doublet must be added in order to give the $\tau_3 = 1$ components of the $SU(2)$ fermion doublets mass. The mechanism of the symmetry breaking is very similar to that of the standard model except there are two Higgs doublets.[76, 77] Before the symmetry breaking there are two complex scalar $SU(2)$ doublets, Φ_1 and Φ_2, for a total of 8 degrees of freedom. When the spontaneous symmetry breaking

[17] Φ^c cannot be written as a chiral superfield.

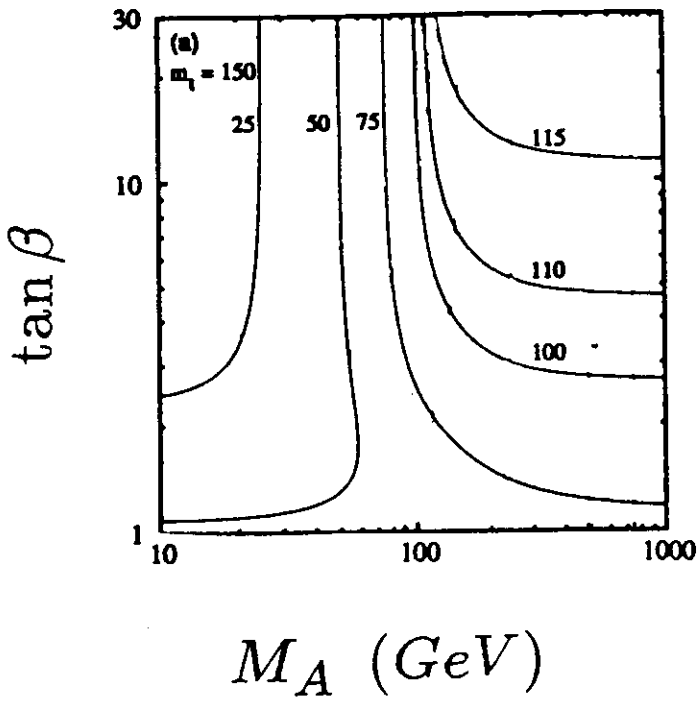

Figure 40: Mass of the lightest Higgs boson of a SUSY model (in GeV) in terms of $\tan\beta$ and M_A for $M_T = 150\ GeV$. This figure is from Ref. [80].

occurs, each scalar obtains a VEV, v_1 and v_2, and the theory is described in terms of the ratio of VEVs,

$$\tan\beta \equiv \frac{v_2}{v_1}. \tag{131}$$

In order that the W mass have the observed value we have the restriction, $v \equiv \sqrt{v_1^2 + v_2^2} = 246\ GeV$.

After the spontaneous symmetry breaking the $W^{\pm}$ and Z get their longitudinal components as in the Standard Model and there are 5 remaining degrees of freedom. Supersymmetric models, therefore, have 5 physical Higgs bosons: 2 neutral scalars, H_1 and H_2, 2 charged scalars,$H^{\pm}$, and a pseudoscalar, A^0. Because of the supersymmetry, the scalar potential has only one free parameter (unlike the case of the general two Higgs doublet model where the scalar potential depends on 6 unknown parameters[78]). The masses of the Higgs scalars can thus be expressed in terms of two parameters which are conventionally taken to be the mass of the pseudoscalar, M_A, and $\tan\beta$.[18] This gives relationships between the masses of the SUSY Higgs particles. The tree level relationships between the SUSY scalar masses, however, receive large radiative corrections at one-loop of $\mathcal{O}(M_T^4/M_W^4)$.[79] In Fig. 40, we show the mass of the lightest neutral Higgs boson in terms of $\tan\beta$ and M_A.[80] There is an upper bound to the mass of the lightest Higgs boson which depends on the top quark mass through the radiative corrections,

$$M_{H_1}^2 < M_Z^2 + \frac{3G_F}{\sqrt{2}\pi^2} M_T^4 \log\left(1 + \frac{\tilde{m}^2}{M_T^2}\right) \tag{132}$$

[18]Remember that in the Standard Model, there was only one free parameter, M_H.

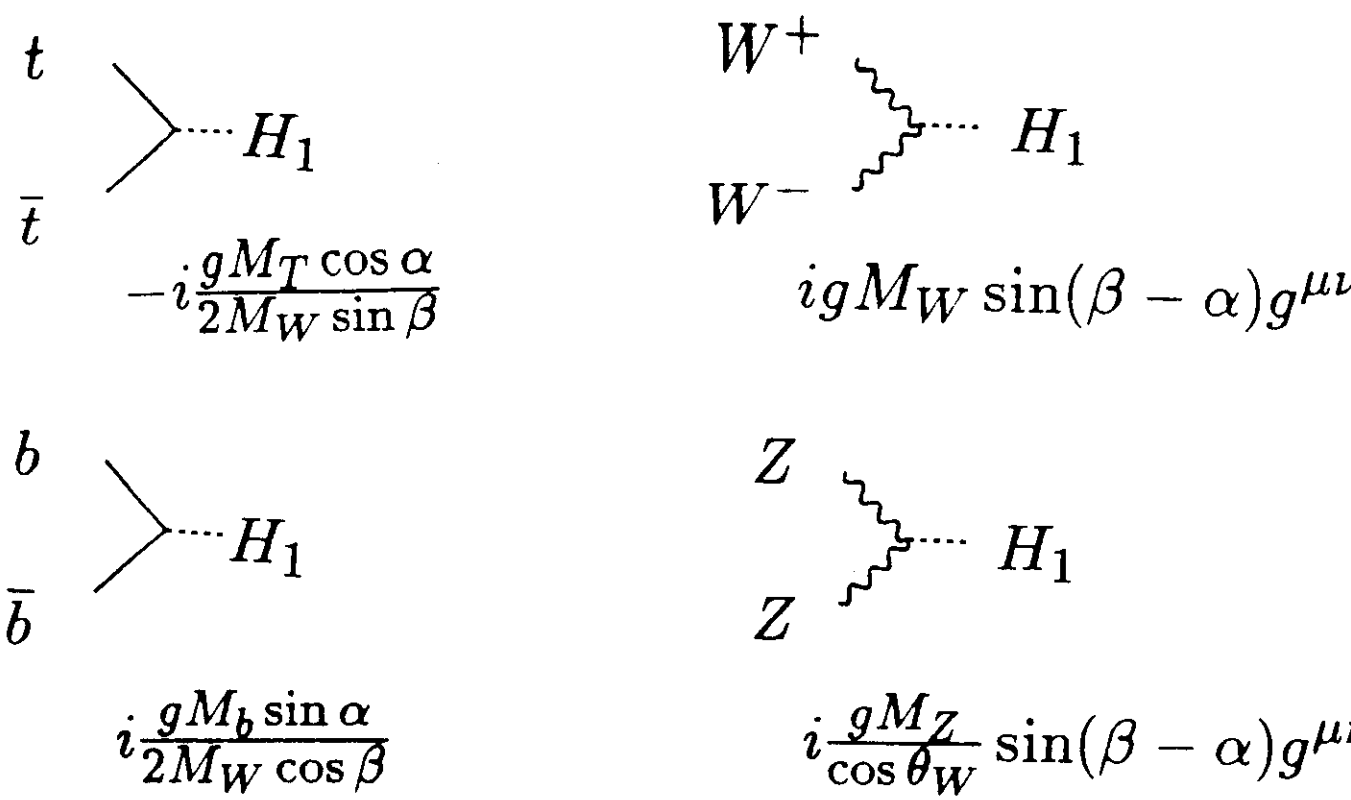

Figure 41: Couplings of the lightest SUSY Higgs boson, H_1, to the Z.

where $\tilde{m}$ is the scale associated with the supersymmetry breaking, usually taken to be $\sim 1\ TeV$. For $M_T \sim 170\ GeV$,[79]

$$M_{H_1} \lesssim 120\ GeV. \tag{133}$$

Hence in a SUSY model, the Higgs mechanism can be excluded experimentally if a Higgs boson is not found below this mass scale. This is in direct contrast to the Standard Model where there is no prediction for the Higgs boson mass.

There are several relevant features for SUSY phenomenology. The first is that the couplings of the neutral scalars to vector bosons ($V = W^{\pm}, Z$) are suppressed from those of the standard model

$$g^2_{H_1VV} + g^2_{H_2VV} = g^2_{HVV}(SM) \tag{134}$$

where g_{HVV} is the coupling of the Higgs boson to vector bosons. Because of this sum rule, the WW scattering production mechanism tends not to be as important in SUSY models as in the Standard Model.

The couplings of the lightest Higgs boson to the Z are shown in Fig. 41. The processes $e^+e^- \to ZH_1$ and $e^+e^- \to A^0H_1$ can be seen from Fig. 41 to be complementary in a SUSY model: they cannot be simultaneously suppressed. Using the 2 modes the e^+e^- machines can cover the SUSY parameter space without holes. In Fig. 42 we show the range of parameter space which has been excluded by the ALEPH experiment at LEP.[81] They find:

$$\begin{aligned} M_{H_1} &> 43\ GeV \\ M_A &> 21\ GeV. \end{aligned} \tag{135}$$

Of course for a given value of M_{H_1} or M_A there may be a stronger limit than Eq. 135.

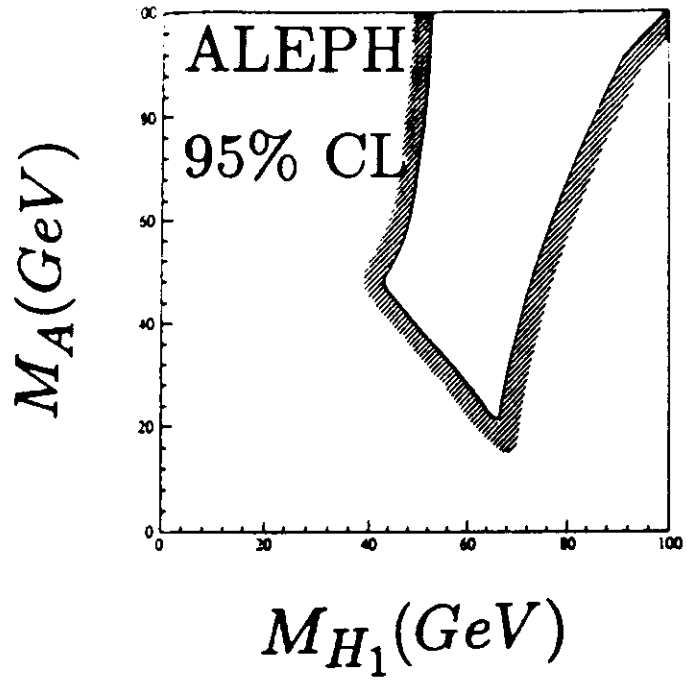

Figure 42: Limits on SUSY parameter space from ALEPH [81]

The second important feature for the phenomenology of SUSY models is that fermion couplings are no longer strictly proportional to mass. The neutral Higgs boson couplings to fermions are:

$$\begin{aligned}\mathcal{L}_{Hff} &= -\frac{gm_d}{2M_W\cos\beta}\bar{d}d\Big(H_2\cos\alpha - H_1\sin\alpha\Big) \\ &\quad -\frac{gm_u}{2M_W\sin\beta}\bar{u}u\Big(H_2\sin\alpha + H_1\cos\alpha\Big) \\ &\quad +\frac{igm_d\tan\beta}{2M_W}\bar{d}\gamma_5 dA^0 + \frac{igm_u\cot\beta}{2M_W}\bar{u}\gamma_5 uA^0 \end{aligned} \tag{136}$$

where α is a mixing angle in the neutral Higgs sector,

$$\begin{aligned} H_2 &= \sqrt{2}\Big[(Re\Phi_1^0 - v_1)\cos\alpha + (Re\Phi_2^0 - v_2)\sin\alpha\Big] \\ H_1 &= \sqrt{2}\Big[-(Re\Phi_1^0 - v_1)\sin\alpha + (Re\Phi_2^0 - v_2)\cos\alpha\Big] \end{aligned} \tag{137}$$

At a hadron collider, the neutral SUSY higgs bosons can be searched for using the same techniques as in the standard model. For most choices of the parameter space, gluon fusion is the dominant production mechanism. In the Standard Model, it was only the top quark contribution to gluon fusion which was important. In a SUSY model, however, the coupling to the b quark can be important for small values of $\cos\beta$, as can be seen from Eq. 136.

SUSY models have a rich particle spectrum in which to search for evidence of the Higgs mechanism. The various decays such as $H_i \to \gamma\gamma$, $H^+ \to l^+\nu$, $A^0 \to \tau^+\tau^-$, etc, are sensitive to different regions in the $M_A - \tan\beta$ parameter space. It takes the combination of many decay channels in order to be able to cover the parameter space

completely with out any holes. Discussions of the capabilities of the LHC detectors to experimentally observe evidence for the Higgs bosons of SUSY models can be found in the ATLAS[18] and CMS[19] studies.

9 Conclusions

Our current experimental knowledge of the Higgs boson gives only the limits $M_H > 58\ GeV$ found from direct searches and $M_H < 780\ GeV$ from precision measurements at the LEP experiments. The lower limit will be extended to a mass reach on the order of 80 GeV at LEPII. From here, we must wait until the advent of the LHC for further limits. Through the decay $H \rightarrow \gamma\gamma$ and the production process $pp \rightarrow Zl^+l^-$, the LHC will probe the mass region between $100 < M_H < 180\ GeV$. It is an important question as to whether there will be a hole in the Higgs mass coverage between the upper reach of LEPII and the lower reach of the LHC. Current ideas as to how to look for a Higgs boson in this mass regime focus on the production mechanism, $pp \rightarrow WH$, with $H \rightarrow b\bar{b}$. The efficiency of this technique, however, depends sensitively on the capabilities of the LHC to do b tagging at a high luminosity. For the higher mass region, $180 < M_H < 800\ GeV$, the LHC will be able to see the Higgs boson through the gold plated decay mode, $H \rightarrow ZZ \rightarrow l^+l^-l^+l^-$.

One of the important yardsticks for all current and future accelerators is their ability to discover (or to definitively exclude) the Higgs boson of the Standard Model. We hope that at the time of the LHC, we will be able to probe all mass scales up to $M_H \sim 800\ GeV$. If the Higgs boson is not found below this mass scale then we are in the regime where perturbative unitarity has broken down and we are led to the exciting conclusion that there must be new physics beyond the Standard Model waiting to be discovered.

References

[1] J. Gunion, H. Haber, G. Kane, and S. Dawson, *The Higgs Hunters Guide*, (Addison-Wesley, Menlo Park, 1990).

[2] Similar material can be found in J. Bagger, TASI 1991, (World Scientific, Singapore, 1991); A. Djouadi, U.de.M-Gpp-TH-94-01, 1994.

[3] An introduction to the standard model can be found in C. Quigg, *Gauge Theories of the Strong, Weak, and Electromagnetic Interactions*, (Benjamin-Cummings, Reading, MA., 1983).

[4] P. W. Higgs, *Phys. Rev. Lett.* **13** (1964)508; *Phys. Rev.* **145** (1966) 1156; F. Englert and R. Brout, *Phys. Rev. Lett.* **13** (1964) 321; G. S. Guralnik, C. R. Hagen, and T. Kibble, Phys. Rev. Lett. **13** (1965) 585; T. Kibble, *Phys. ReV.* **155** (1967) 1554.

[5] E. Abers and B. Lee, *Phys. Rep.* **9** (1975) 1.

[6] S. Glashow, *Nucl. Phys.* **22** (1961) 579; S. Weinberg, *Phys. Rev. Lett.* **19** (1976) 1264; A. Salam, in *Elementary Particle Theory*, ed. N. Svartholm (Almqvist and Wiksells, Stockholm, 1969), p. 367.

[7] R. Peccei, lectures presented at this school.

[8] J.Bjorken, in *Proc. of the 1976 SLAC Summer Institute on Particle Physics*, (Stanford, CA., 1976), Ed. M. Zipf, p.1; F. Berends and R. Kleiss, *Nucl. Phys.* **B260** (1985) 32.

[9] *Review of Particle Properties*, *Phys. Rev.* **D50** (1994) 1.

[10] T. Mori, *Proc. of the XXVI International Conference on High Energy Physics*, (Dallas, Texas, 1992), Ed. J. Sanford, p. 1321.

[11] B. Ioffe and V. Khoze, *Sov. J. Part. Nucl. Phys.* **9** (1978) 50; B. W. Lee, C. Quigg, and H. B. Thacker, *Phys. Rev.* **D16** (1977) 1519.

[12] W. Marciano, *Phys. Rev.* **D12** (1975) 3861; G. t'Hooft and M. Veltman, *Nucl. Phys.* **B153** (1979) 365 .

[13] F. Wilczek, *Phys. Rev. Lett.* **39** (1977) 1304; J. Ellis *et.al.*, *Phys. Lett.* **83B** (1979) 339; H. Georgi *et. al.*, *Phys. Rev. Lett.* **40** (1978) 692; T. Rizzo, *Phys. Rev.* **D22** (1980) 178.

[14] R. Cahn,*Proc. of the 1982 SLAC Summer Institute*, Stanford, CA., 1982.

[15] T. Appelquist and J. Carrazone, *Phys. Rev.* **D11** (1975) 2856.

[16] S. Dawson and R. Kauffman, *Phys. Rev.* **D** (1994); A. Djouadi, M. Spira and P. Zerwas, *Phys. Lett.* **B264** (1991) 441.

[17] P. Agrawal and S. Ellis, *Phys. Lett.* **B229** (1989) 145.

[18] LOI of the ATLAS Collaboration, CERN/LHCC/92-4, Oct., 1992.

[19] LOI of the CMS Collaboration, CERN/LHCC/92-3, Oct., 1992.

[20] J. Gunion, G. Kane, and J. Wudka, *Nucl. Phys.* **B299** (1988) 231.

[21] U. Baur and E. Glover, *Nucl. Phys.* **B347** (1990) 12; *Phys. Rev.* **D44** (1991) 99.

[22] An excellent introduction to the parton model is given in S. Willenbrock, TASI,1990 (World Scientific, Singapore, 1990). Note the typographical error in the limits of Eq. 12.6 of this paper.

[23] K. Ellis *et.al.*, *Nucl. Phys.* **B297**(1988) 221.

[24] E. Braaten and J. Leveille, *Phys. Rev.* **D22** (1980) 715; M. Drees and K. Hikasa, *Phys. Lett.* **B240** (1990) 455.

[25] A. Vainshtein *et.al.*, *Sov. J. Nucl. Phys.*; M. Voloshin, *Sov. J. Nucl. Phys.* **B44** (1986) 478.

[26] J. Morfin and W. Tung, *Z. Phys.* **C52** (1991) 13.

[27] W. Marciano, A. Stange, and S. Willenbrock, *Phys. Rev.* **D49** (1994) 1354.

[28] J. Gunion and T. Han, UCD-94-10,1994.

[29] S. Dawson and S. Willenbrock, *Phys. Rev.* **D40** (1989); M. Veltman and F. Yndurain, *Nucl. Phys.* **B163** (1979) 402.

[30] S. Brodsky, T. Kinoshita, and H. Terazawa, *Phys. Rev.* **D4** (1971) 1532.

[31] S. Dawson, *Nucl. Phys.* **B249** (1985) 42; G. Kane, W. Repko, and W. Rolnick, *Phys. Lett* **B148** (1984) 367; M Chanowitz and M. Gaillard, *Phys. Lett.* **B142** (1984) 85.

[32] J. Lindfors, *Z. Phys.* **C28** (1985) 427.

[33] S. Dawson and J. Rosner, *Phys. Lett.*, **B148** (1984) 497.

[34] Z. Kunszt and D. Soper, *Nucl. Phys.* **B272** (1988) 253.

[35] T. Han, S. Willenbrock, and G. Valencia, *Phys. Rev. Lett.* **69** (1992) 3274; S. Dawson, *Phys. Lett.* **B217** (1989) 347.

[36] D. Dicus and R. Vega, *Phys. Rev. Lett* **57** (1986) 1110.

[37] A. Abbasabadi *et.al.* , *Phys. Rev.* **D38** (1988) 2770.

[38] J. Gunion, J. Kalinowski, and A. Tofighi-Niaki, *Phys. Rev. Lett.* **57** (1988) 2351.

[39] W. Kunszt, *Nucl. Phys.* **B247** (1984) 339; W. Marciano and F. Paige, *Phys. Rev. Lett.* **66** (1991) 2433; J. Gunion, *Phys. Lett.* **B261** (1991) 510 .

[40] I thank A. Stange for this figure.

[41] R. Cahn *et. al. Phys. Rev.* **D35** (1987) 1626; V. Barger, T. Han, and R. Phillips, *Phys. Rev.* **D37** (1988) 2005; J. Gunion and M. Soldate, *Phys. Rev.* **D34** (1986) 826.

[42] M. Chanowitz, M. Furman, and I. Hinchliffe, *Nucl. Phys.* **B153** (1979) 402.

[43] B. Lee, C. Quigg, and H. Thacker, *Phys. Rev.* **D16** (1977) 1519; D. Dicus and V. Mathur, *Phys. Rev.* **D7** (1973) 3111.

[44] M. Duncan, G. Kane, and W. Repko, *Nucl. Phys.* **B272** (1986) 517.

[45] J. Cornwall, D. Levin, and G. Tiktopoulos, *Phys. Rev.* **D10** (1974) 1145; **D11** (1975) 972E; B. Lee, C. Quigg, and H. Thacker, *Phys. Rev.* **D16** (1977) 1519; M. Chanowitz and M. Gaillard, *Nucl. Phys.* **B261** (1985) 379; Y.-P. Yao and C. Yuan, *Phys. Rev.* **D38** (1988) 2237; J. Bagger and C. Schmidt, *Phys. Rev.* **D41** (1990) 264; H. Veltman, *Phys. Rev.* **D41** (1990) 2294.

[46] W. Marciano and S. Willenbrock, *Phys. Rev.* **D37** (1988) 2509.

[47] J. Gasser and H. Leutwyler, *Ann. Phys.* **158** (1984) 142; *Nucl. Phys.* **B250** (1985) 465.

[48] M. Chanowitz, H. Georgi, and M. Golden, *Phys. Rev. Lett.* **57** (1986) 2344; *Phys. Rev.***D36** (1987) 1490.

[49] T. Appelquist and C. Bernard, *Phys. Rev.* **D22** (1980) 200; A. Longhitano, *Nucl. Phys.* **B188** (1981) 118.

[50] S. Weinberg, *Phys. Rev. Lett.* **17** (1966) 616.

[51] R. Brown, D. Sahdev, and K. Mikaelian, *Phys. Rev.* **D20** (1979) 1164; W. Alles, C. Boyer, and A. Buras, *Nucl. Phys.* **B119** (1977) 125.

[52] S. Dawson and G. Valencia, *Nucl. Phys.* **B348** (1991) 23.

[53] B. Holdom, *Phys. Lett.* **B258** (1991) 156.

[54] S. Dawson and G. Valencia, BNL-60949, 1994.

[55] M. Peskin and T. Takeuchi, *Phys. Rev. Lett.* **65** (1990) 964; D. Kennedy and B. Lynn, *Nucl. Phys.* **B322** (1989) 1.

[56] S. Dawson and G. Valencia, *Nucl. Phys.***B352** (1991) 27 ;F. Boudjema, *Proc. of Physics and Experiments with Linear e^+e^- Colliders*, ed. F. Harris *et. al.*, (1993), p. 713; A. Dobado, M. Herrero and T. Truong, *Phys. Lett.* **B253** (1990) 129; M. Chanowitz and M. Golden, *Phys. Rev. Lett.* **61** (1988) 1053; **(E)63** (1989) 466; M. Chanowitz and W. Kilgore, *Phys. Lett.* **B322** (1994) 147; M. Berger and M. Chanowitz, *Phys. Lett.* **B263** (1991) 509; V. Koulovassilopoulos and R. Chivukula, *Phys. Rev.* **D** (1994) 3218.

[57] P. Langacker, Invited talk presented at the 22nd INS Symposium on Physics with High Energy Colliders, Tokyo, March, 1994, UPR-0624T.

[58] J. Donoghue, C. Ramirez, and G. Valencia, *Phys. Rev.* **D38** (1988) 2195; *Phys. Rev.* **D39** (1989) 1947; M. Herrero and E. Morales, *Nucl. Phys.* **B418** (1993) 364.

[59] J. Bagger, S. Dawson, and G. Valencia, *Nucl. Phys.* **B399** (1993) 364.

[60] A. Falk, M. Luke, and E. Simmons, *Nucl. Phys.* **B365** (1991) 523; U. Baur *et.al.*, FSU-HEP-941010, 1994.

[61] J. Bagger *et.al.*, *Phys. Rev.* **D49** (1994) 1246.

[62] M. Chanowitz and M. Gaillard, *Nucl. Phys.* **B261** (1985) 379.

[63] K. Wilson, *Phys. Rev.* **B4** (1971) 3184; K. Wilson and J. Kogut, *Phys. Rep.* **12** (1974) 75.

[64] R. Dashen and H. Neuberger, *Phys. Rev. Lett.* **50** (1983) 1897; P. Hasenfratz and J. Nager, *Z. Phys.* **C37** (1988); J. Kuti, L. Lin, and Y. Shen, *Phys. Rev. Lett.* **61** (1988) 678; M. Luscher and P. Weisz, *Phys. Lett.* **B212** (1988) (472).

[65] A. Hasenfratz, *Quantum Fields on the Computer*, Ed. M. Creutz, (World Scientific, Singapore, 1992),p. 125.

[66] T. Cheng, E. Eichten and L. Li, *Phys. Rev.* **D9** (1974) 2259; B. Pendleton and G. Ross, *Phys. Lett.* **B98** (1981) 291; C. Hill, *Phys. Rev.* **D24** (1981) 691; J. Bagger, S. Dimopoulos and E. Masso, *Nucl. Phys.* **B253** (1985) 397; M. Beg, C. Panagiotakopoulos, and A. Sirlin, *Phys. Rev. Lett.* **52** (1984) 883; M. Duncan, R. Philippe, and M. Sher, *Phys. Lett.* **B153** (1985) 165; K. Babu and E. Ma, *Phys. Rev. Lett.* **55** (1985) 3005.

[67] N. Cabibbo *et.al.*, *Nucl. Phys.* **B158** (1979) 295.

[68] A. Linde, *JETP Lett* **23** (1976) 64; *Phys. Lett.* **B62** (1976) 435; S. Weinberg, *Phys. Rev. Lett.* **36** (1976) 294; S. Coleman and E. Weinberg, *Phys. Rev.* **D7** (1973) 188.

[69] M. Lindner, M. Sher, and H. Zaglauer, *Phys. Lett.* **B228** (1989) 139; C. Ford *et. al.*, *Nucl. Phys.* **B395** (1993) 62; M. Sher, *Phys. Rep.* **179** (1989)274; F. del Aguila, M Martinez, M. Quiros, *Nucl. Phys.* **B381** (1992) 451.

[70] M. Sher, *Phys. Lett.* **B317** (1993)159; addendum, **B331** (1994) 448.

[71] W. Marciano and A. Sirlin, *Phys. Rev. Lett.* **46** (1981) 163; W. Marciano, S. Sarantakos, and A. Sirlin, *Nucl. Phys.* **B217** (1988) 84.

[72] M. Veltman, *Acta. Phys. Pol.* **B8** (1977) 475.

[73] M. Einhorn and J. Wudka, *Phys. Rev.* **D339** (1989) 2758.

[74] P. Langacker, TASI 1992, (World Scientific, Singapore, 1992).

[75] T. Appelquist, lectures presented at this school.

[76] P. Ramond, lectures presented at this school.

[77] For a review of SUSY phenomenology, see G. Kane and H. Haber, *Phys. Rep.* **117C** (1985) 75; H. Haber, TASI 1992 (World Scientific, Singapore, 1992).

[78] G. Kane, H. Haber, and T. Stirling, *Nucl. Phys.* **B161** (1979) 493.

[79] H. Haber and R. Hempfling, *Phys. Rev. Lett.* **66** (1991) 1815; J. Ellis, G. Ridolfi and F. Zwirner, *Phys. Lett.* **B257** (1991) 83; M. Berger, *Phys. Rev.* **D41** (1990) 225; Y. Okada, M. Yamaguchi, and T. Yanagida, *Prog. Theor. Phys. Lett.* **85** (1991)1.

[80] V. Barger *et.al.*, *Phys. Rev.* **D46** (1992) 4914.

[81] G. Wormser, *Proc. of the XXVI International Conference on High Energy Physics*, (Dallas, Texas, 1992), p. 1309; D. Decamp *et.al.*, *Phys. Rep.* **216** (1992) 253.